

Decoding the Entanglement Structure of Monitored Quantum Circuits

Beni Yoshida

Perimeter Institute for Theoretical Physics, Waterloo, Ontario N2L 2Y5, Canada

Abstract

Given an output wavefunction of a monitored quantum circuit consisting of both unitary gates and projective measurements, we ask whether two complementary subsystems are entangled or not. For Clifford circuits, we find that this question can be mapped to a certain classical error-correction problem where various entanglement measures can be explicitly computed from the recoverability. The dual classical code is constructed from spacetime patterns of out-of-time ordered correlation functions among local operators and measured Pauli operators in the past, suggesting that the volume-law entanglement in a monitored circuit emerges from quantum information scrambling, namely the growth of local operators. We also present a method of verifying quantum entanglement by providing a simple deterministic entanglement distillation algorithm, which can be interpreted as decoding of the dual classical code. Discussions on coding properties of a monitored Clifford circuit, including explicit constructions of logical and stabilizer operators, are also presented. Applications of our framework to various physical questions, including non-Clifford systems, are discussed as well. Namely, we argue that the entanglement structure of a monitored quantum circuit in the volume-law phase is largely independent of the initial states and past measurement outcomes except recent ones, due to the decoupling phenomena from scrambling dynamics, up to a certain polynomial length scale which can be identified as the code distance of the circuit. We also derive a general relation between the code distance and the sub-leading contribution to the volume-law entanglement entropy. Applications of these results to black hole physics are discussed as well.

Contents

1	Introduction	4
1.1	Previous works	5
1.2	Main results	7
1.2.1	Entanglement structure (Section 3, 4, 5)	7
1.2.2	Coding properties (Section 6, 7, and Appendix E)	8
1.2.3	Hierarchy of entanglement structure (Section 8, 9)	9
1.2.4	Other applications (Section 10, 11)	10
2	Monitored quantum circuit as sequential measurements	10
3	Dual classical error-correction problem	12
3.1	Codeword and error vectors	13
3.2	Classical error-correcting code	14
3.3	Entanglement structure from classical error-correction	15
3.4	Examples	16
3.4.1	Commuting P_j 's	17
3.4.2	Non-commuting P_j 's (recoverable)	18
3.4.3	Non-commuting P_j 's (not recoverable)	18
4	Entanglement distillation between two subsystems	19
4.1	Perfect distillation	19
4.2	Imperfect distillation	21
4.3	Examples	22
4.3.1	No measurement	22
4.3.2	Single-qubit measurement	22
4.3.3	Two-qubit measurement	23
4.3.4	Two-qubit commuting measurement	24
4.3.5	Two-qubit non-commuting measurement	24
4.4	Distillation algorithm for the Gullans-Huse proposal	25
5	Operator growth in spacetime	26
6	Coding properties of monitored Clifford circuit	27
6.1	System-Reference entanglement	28
6.2	Stabilizer group	29
6.3	Logical operators	30
6.4	Examples	31
7	Distilling the Choi-Jamiołkowski state	32
7.1	Reverse error vector	33
7.2	Choi-Jamiołkowski state	34

8	State-independent entanglement structure	35
8.1	Decoupling and state-independence	35
8.2	Estimate of the code distance	36
8.3	Measurement history dependence	37
9	State-dependent entanglement structure	38
9.1	Entanglement swapping by random projection	38
9.2	On complexity of entanglement verification	40
9.3	Does measurement destroy entanglement?	41
10	Code distance from sub-leading entropy	42
11	Relation to black hole physics	44
12	Outlook	46
A	Measurement probability (Proof of lemma 1)	48
A.1	Measurement probability	48
A.2	Summation of measurement probability	50
A.3	Proof of lemma 9	50
B	Output of distillation algorithm (Proof of lemma 2)	54
B.1	No feedback	54
B.2	With feedback	55
B.3	Imperfect cases	55
C	Conditional entropy (Proof of theorem 2)	57
D	Logical operators (Proof of lemma 4)	59
E	More on coding properties	60
E.1	Extended codewords	60
E.2	Stabilizer operator from extended code	61
E.3	Cleaning lemma for monitored circuit	62
E.4	Measurement probability (Proof of lemma 5)	63
E.5	Entanglement distillation from reference (Proof of lemma 6)	64

1 Introduction

Recently it has been discovered that monitored quantum circuits consisting of both interacting unitary dynamics and local projective measurements can retain long-range entanglement obeying the volume-law [1, 2]. These theoretical findings hint far-reaching possibility that quantum entanglement may play crucial roles in the physics of many-body quantum systems outside controlled laboratory setups where the systems are continuously monitored by observers and decohere to the environment. Indeed, it is illuminating to remind ourselves that objects surrounding our daily lives, such as a cup of coffee, are after all quantum many-body systems which evolve unitarily in the presence of continuous measurements. However, if entanglement in monitored quantum systems would ever be relevant to naturally occurring and observable physical phenomena, the entanglement must be verifiable by some simple physical processes since observing such phenomena would verify the entanglement. While previous studies on monitored quantum circuits have revealed interesting features of entanglement phase transitions driven by measurement rates (see [3–14] for samples of previous works), our current understanding of the *entanglement structure* arising in a monitored quantum circuit remains elusive with no known universal method of verifying quantum entanglement.

In this paper, we investigate the entanglement structure arising in a monitored quantum circuit. We will pay particular attention to the following three key questions.

- (a) **Entanglement Structure:** Given an output wavefunction of a monitored quantum circuit, how is a subsystem A entangled with its complementary subsystem B ?
- (b) **Entanglement distillation:** When two subsystems A and B are entangled with each other, how do we verify their entanglement? Specifically, how do we distill simple entangled states (such as EPR pairs) from A and B ?
- (c) **Measurement dependence**¹: How does the entanglement structure of a monitored quantum circuit depend on measurement results in the past? To what extent do measurement outcomes in the past influence the entanglement structure? Relatedly, does the entanglement depend on the initial states of the circuit?

In this paper, we will address these questions by focusing on monitored quantum circuits whose unitary part of the dynamics are supplied by Clifford operators, which are unitary operators that transform Pauli operators to (possibly different) Pauli operators. While Clifford dynamics differs from generic dynamics of interacting many-body quantum systems in crucial ways, Clifford dynamics can teach us qualitative features of entanglement structure that are universal for monitored quantum circuits. Our goal is to develop a theoretical tool to understand the entanglement structure arising in a monitored Clifford circuit and propose a simple entanglement distillation algorithm that verifies quantum entanglement between two subsystems A and B . Building on these results on monitored Clifford circuits, we will obtain some physical implications which can be applied widely to generic monitored quantum circuits.

¹The entanglement structure of a monitored quantum circuit depends on the measurement outcomes in the past, as well as the initial states of the circuit, until these are forgotten after an exponentially long time-evolution. One might then expect that verifying the entanglement requires knowledge of measurement outcomes in the distant past. The nature, however, would not be keeping a record of exponentially many measurement outcomes and utilize them cleverly to verify the entanglement. Hence, if the entanglement arising in a monitored many-body quantum system is to be relevant to some observable phenomena, it should *not* depend on measurement outcomes in the distant past or the initial states. In this paper, we will argue that this is indeed the case below a certain length scale.

1.1 Previous works

The central challenge is to reveal the entanglement structure, namely to understand how two subsystems are entangled in the output wavefunction of a monitored circuit. This question can be addressed unambiguously by solving the *entanglement distillation problem*. Loosely speaking, if two subsystems A and B are entangled with each other, one should be able to distill quantum entanglement between A and B and convert it into some “usable” or “simple” forms of entangled states, such as an EPR pair $\frac{1}{\sqrt{2}}(|00\rangle + |11\rangle)$, by acting only on A and B locally. Entanglement distillation typically requires us to localize the entangled degrees of freedom on A and B into locally supported qubits. This is what we mean by understanding and verifying the entanglement structure ².

One possible approach toward the entanglement verification is to interpret the entanglement distillation as a decoding problem and use the Petz recovery map by viewing the output wavefunction as a quantum channel from A to B via the Choi-Jamiołkowski isomorphism [15, 16]. However, the Petz map is a quantum operation that does not necessarily have simple physical realizations. Indeed, its physical implementation typically requires post-selection or amplitude amplification (*i.e.* use of the Grover search algorithm) which may not be physically simple or computationally efficient, especially when the subsystem A becomes large [17].

Another interesting approach toward characterization of the volume-law entanglement is to interpret a monitored quantum circuit as a quantum error-correcting code [18–22]. Namely, instead of starting from a pure state, maximally mixed states are prepared as the initial states. By purifying the system with an ancilla reference system R which is entangled with the original system, the circuit can be viewed as a quantum error-correcting code where the system stores quantum information as entanglement between the system and the reference. The key observation is that the volume-law entanglement is protected from local projective measurements via quantum error-correction [18]. Recent studies have also numerically verified that entanglement phase transition can be addressed by studying the coding properties of a monitored quantum circuit.

Despite its conceptual novelty, the quantum error-correction approach has a crucial drawback of not being a direct measure of quantum entanglement arising in a monitored quantum system itself. Indeed, it remains puzzling why the entanglement between the system and the reference R may serve as a probe of the entanglement within the system. Verification of the entanglement between the system and the reference is also a non-trivial task. Another issue is that the quantum memory, stored in a monitored circuit, will be eventually lost after an exponentially long time-evolution [19, 23]. Yet, the volume-law entanglement from a monitored quantum circuit remains even after the circuit loses its initial quantum information. Here we hope to understand universal signatures of the entanglement structure in a monitored quantum circuit which is independent of the reference system R and is applicable at any given moment, including moments after an exponentially long time-evolution.

Another interesting approach is to simulate a monitored circuit by a unitary circuit without measurements via a certain spacetime duality [24].

²One might think of preparing two copies of the output wavefunctions and measure the Rényi-2 entropy. But finding the (naive Rényi-2 generalization of) mutual information, for instance, requires us to find $S_B^{(2)}$ by measuring $\text{Tr}(\rho_B^2)$ which will be exponentially small in most of the interesting cases. In addition, preparing identical copies will be even more difficult for monitored systems since measurement outcomes in two copies must be identical as well.

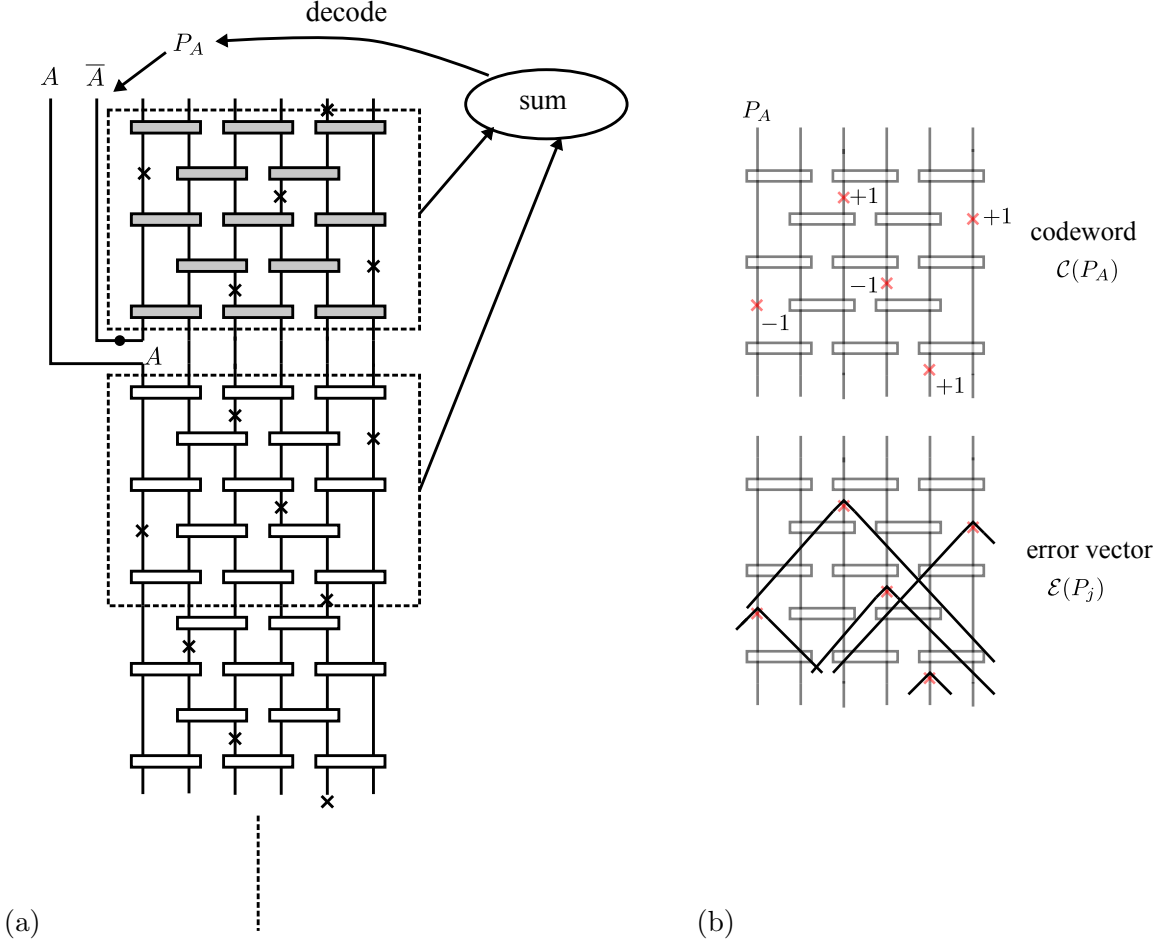


Figure 1: (a) A summary of the entanglement distillation algorithm. Given an output wavefunction of a monitored Clifford circuit, we insert additional EPR pairs on A and \bar{A} (shown as a horizontal line with a black dot). We then implement the same measurement sequence in a reverse order (shown in shaded blocks). A sum of the original and reverse measurement results m and \bar{m} generates a bit string $s = m \cdot \bar{m}$. Based on the bit string s , we apply some feedback Pauli operator P_A . An appropriate feedback operation can be found by error-correcting this bit string s into a codeword bit string $\mathcal{C}(P_A)$. As shown in the figure, one needs to reverse only a part of the original monitored circuit since measurement histories in the distant past will not influence the entanglement between A and B due to the decoupling phenomena arising from scrambling dynamics. (b) Construction of a dual classical error-correcting code. Here the codeword $\mathcal{C}(P_A)$ records the space-time pattern of the operator growth of P_A as OTOCs with respect to local Pauli operators which were projectively measured in the past. Error vectors $\mathcal{E}(P_j)$ corresponds to OTOCs between a measured Pauli operator P_j and other measured Pauli operators in the past.

1.2 Main results

1.2.1 Entanglement structure (Section 3, 4, 5)

In this paper, we develop a theoretical framework to investigate the entanglement structure arising in a monitored Clifford circuit and present an entanglement distillation algorithm that verifies quantum entanglement in two complementary subsystems. The main results are summarized as follows. (See Fig. 1).

- (a) **Dual classical code problem:** We will show that the problem of revealing the entanglement structure of a monitored Clifford circuit can be mapped to a certain *classical error-correction problem* where the recoverability of initial classical information corresponds to the presence of entanglement between two subsystems A and B .
- (b) **Entanglement distillation algorithm:** We will present a simple deterministic algorithm to distill EPR pairs from two complementary subsystems A and B . The algorithm can be interpreted as a decoding procedure of the dual classical error-correcting code.

We will begin by showing that a certain dual classical error-correction problem can be employed to study the entanglement structure of a monitored Clifford circuit. The corresponding classical code is constructed by examining commutation relations among local Pauli operators on a subsystem A and measured Pauli operators P_j in the past. Given a Pauli operator P_A on a subsystem A , we think of encoding P_A into a codeword vector $\mathcal{C}(P_A)$ by recording its commutation relations with respect to measured Pauli operators P_j . These codeword vector $\mathcal{C}(P_A)$ will be acted by error vectors $\mathcal{E}(P_j)$ which account for commutation relations among measured Pauli operators P_j 's in a certain manner so that causal orderings are taken into account. See Fig. 1(b). The central result is that two subsystems A and B are maximally entangled if and only if the initial information P_A can be recovered even when error vectors $\mathcal{E}(P_j)$ act on codeword vectors $\mathcal{C}(P_A)$. In other words, the recoverability of the dual classical error-correcting code serves as a necessary and sufficient condition for maximal quantum entanglement between A and B . In fact, by studying how much of classical information remains recoverable, one can explicitly compute the conditional entropy $S_{A|B}$:

$$S_{A|B} \equiv S_{AB} - S_B \quad (1)$$

where the recoverability of the classical code corresponds to the negativity of the conditional entropy. The conditional entropy can be interpreted as the coherent quantum information when we view the output wavefunction as a quantum channel from A to B . As such, the recoverability of the dual classical code underpins the robustness of quantum entanglement in a monitored Clifford circuit.

We then present a deterministic algorithm for distilling quantum entanglement from A and B . The algorithm implements the reverse of the monitored Clifford circuit as shown in Fig. 1. When the measurement outcomes are “favorable”, EPR pairs will be automatically distilled without the need of further actions. When the measurement outcomes are not “favorable”, then some feedback operation is needed. The appropriate feedback operation can be found by solving the decoding problem of the dual classical code. Specifically, letting m and \bar{m} be the vectors which record measurement outcomes in the original circuit and the reverse circuit respectively, the sum vector $s = m \cdot \bar{m}$ plays the central role in the distillation algorithm. Namely, the sum vector s is interpreted as an outcome of applying some error vectors on codeword vectors. By decoding the sum vector s , one can recover the original classical

information which corresponds to some Pauli operator P_A . This P_A is the necessary feedback operator to distill EPR pairs.

We also present an application of this distillation algorithm to a certain proposal by Gullans and Huse which aims at detecting the entanglement phase transition by entangling the system of a monitored Clifford circuit to a single qubit (or a few qubits) [20].

It is well known that, due to the Gottesman-Knill theorem, Clifford circuits can be decoded efficiently. Here it is worth emphasizing that our algorithm is more efficient than these generic treatments.

These findings suggest that entanglement in a monitored quantum circuit emerges from *scrambling dynamics*, namely the growth of local operators on A by backward time-evolution which overlaps non-trivially with measured local operators in the past. Indeed, encoding into codewords of a dual classical error-correcting code can be interpreted as a space-time pattern of the operator growth (or the out-of-time ordered correlation (OTOC) functions). Hence, our results provide a rigorous and concrete argument to support the folklore belief that the scrambling dynamics, in a sense of OTOC functions, is necessary for the emergence of the volume-law entanglement phase in monitored quantum circuits.

1.2.2 Coding properties (Section 6, 7, and Appendix E)

We will also study the coding properties of a monitored Clifford circuit by interpreting it as a quantum error-correcting code entangled with the reference system R . The framework of using a dual classical error-correcting code enables us to study the entanglement between the system and the reference R as well. The main results are summarized as follows.

- (a) **Entanglement between system and reference:** We will derive explicit formulae of entanglement entropies for subsystems involving A , B , and R . We will also present an algorithm to distill an entangled state from the system and the reference R , and show that it is identical to the Choi-Jamiołkowski state of a monitored Clifford circuit viewed as a stabilizer code.
- (b) **Stabilizer and logical operators:** We will present explicit constructions of stabilizer and logical operators by using the dual classical error-correcting code. We will also derive a version of the cleaning lemma for monitored Clifford circuits.

To study the entanglement structure involving the reference, we will utilize the formula for the conditional entropy by viewing A , B , and the whole system AB as input subsystems of the dual code. In this analysis, Pauli operators which become *indistinguishable* from the identity operator play a crucial role:

$$\mathcal{L} \equiv \langle P \in \text{Pauli} : \mathcal{C}(P) \in \mathcal{E} \rangle, \quad \mathcal{E} \equiv \langle \{\mathcal{E}(P_j)\}_{\forall j} \rangle. \quad (2)$$

Such Pauli operators will be referred to as *null operators*. We find that entanglement entropies in subsystems can be written simply in terms of the numbers of null operators. For instance, the mutual information is given by

$$I_{(A,B)} = \log \frac{N_I}{N_{I_A} N_{I_B}} \quad (3)$$

where N_{I_A}, N_{I_B}, N_I represent the numbers of null operators supported on A , B , and the whole system AB respectively.

It turns out that the null operators of the dual classical code play the role of *logical operators*. We will prove this statement by presenting an explicit recipe of recursively constructing stabilizer operators from measured Pauli operators P_j .

We will also present an algorithm to distill an entangled state between the system AB and the reference R . While the algorithm is simple, finding an appropriate feedback operator requires extra caution. In the dual classical code, the error vectors $\mathcal{E}(P_j)$ were constructed by examining commutation relations with other Pauli operators P_i in the past ($i < j$). Here, in order for the entanglement distillation between the system and the reference, we will need to construct the error vectors $\mathcal{E}_{\text{rev}}(P_j)$ in a *reverse chronological order*, namely by examining commutation relations with respect to other Pauli operators P_i in the *future* ($i > j$). The algorithm generates the Choi-Jamiołkowski state of the corresponding stabilizer code, confirming the quantum error-correcting code interpretation of a monitored Clifford circuit.

1.2.3 Hierarchy of entanglement structure (Section 8, 9)

Our results reveal a certain interesting feature of the entanglement structure of a monitored quantum circuit in the volume-law phase. We will argue that the entanglement structure changes drastically when the subsystem A exceeds a certain polynomial size scale that can be identified as the code distance of the circuit (Fig. 2).

- (a) **Below the code distance scale:** The entanglement between A and its complement B is independent of the initial states of the circuit. Furthermore, the entanglement does not depend on measurements that occurred more than the entanglement equilibrium time before.
- (b) **Above the code distance scale:** The entanglement between A and B depends on the initial states as well as measurement outcomes in the distant past. Nevertheless, the value of the entanglement entropy S_A does not depend on the choice of the initial states once the system reaches the entanglement equilibrium.

Our argument is based on a simple observation based on the decoupling phenomena. We expect that the monitored quantum circuit in the volume-law phase will reach the entanglement equilibrium in the $O(L)$ time scale (L being the linear length), and the entanglement with the reference remains stable until an exponentially long quantum memory time. In the entanglement equilibrium, a subsystem A smaller than the code distance will be decoupled from the reference system R , satisfying $I(A, R) \approx 0$. This suggests that any quantum operation acting on R cannot influence the entanglement between A and B . Observe that projecting the reference R onto a product state $|0\rangle^{\otimes n}$ will set the initial state of the circuit as $|0\rangle^{\otimes n}$. Even after this projection, two subsystems A and B should remain entangled in the same manner. Hence, the entanglement structure below the code distance scale is *state-independent*. Furthermore, since the decoupling of A and R occurs in the entanglement equilibrium time, the entanglement between A and B depend only on recent measurement outcomes up to the entanglement equilibrium time in the past.

Above the code distance scale, we will have $I(A, R) \gtrsim 0$ and hence, the entanglement between A and B will be *state-dependent*. The entanglement verification requires knowledge of measurement outcomes in the distant past as well as the initial state, and is expected to be computationally intractable. Nevertheless, we expect that the value of the entanglement entropy S_A will remain independent of the choice of the initial states. Indeed, one can explicitly show that S_A does not change (except small

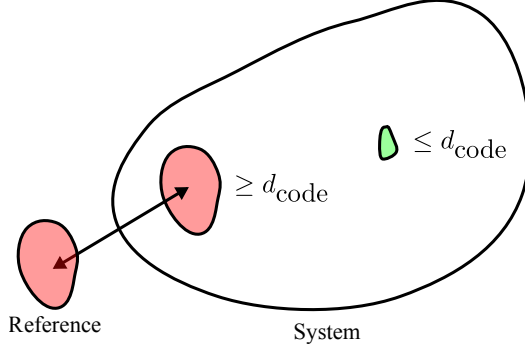


Figure 2: A cartoon of the hierarchy of the entanglement structure. A subsystem smaller than the code distance d_{code} is entangled within the system, and this entanglement does not depend on the measurement outcomes in the distant past or the initial states of the circuit. A subsystem larger than d_{code} is entangled with the reference system as well, and this entanglement is state-dependent.

statistical fluctuations) by choosing a Haar random initial state. Namely, the random projection on R lets the entanglement between A and R join the entanglement between A and B . In the language of quantum information theory, this mechanism is akin to the *entanglement swapping* (or the quantum teleportation) driven by a random projection. As such, the volume-law behavior $S_A \approx a|A|$ persists across the code distance scale regardless of the choice of the initial states even though the nature of the entanglement structure changes drastically.

In order for a monitored quantum circuit to have an exponential quantum memory time, the code distance should scale polynomially with respect to the system size n . As such, the entanglement structure undergoes a transition from being state-independent to being state-dependent at an “intermediate” length scale. We will argue that the above observations can be supported on generic grounds for non-Clifford circuits as well.

1.2.4 Other applications (Section 10, 11)

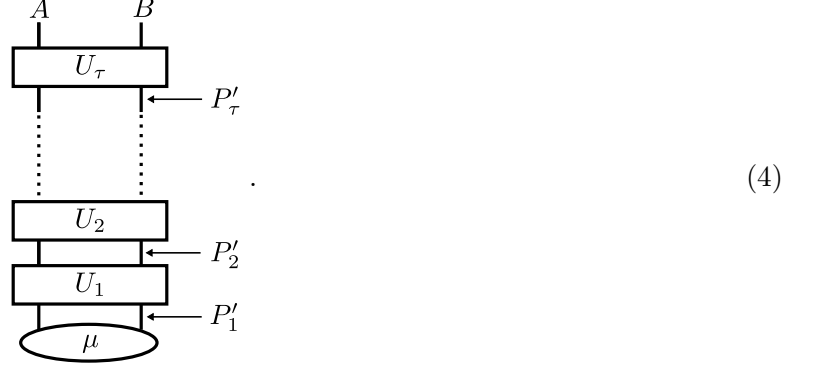
Based on the aforementioned results, we will address two concrete physical questions concerning monitored quantum circuits.

- (a) **Sub-leading contribution:** We will derive a general relation between coding properties of one-dimensional monitored quantum circuits and the sub-leading contribution to the volume-law entanglement entropy. Namely, we will show that, if the code distance scales as $d_{\text{code}} \approx n^{\gamma_{\text{code}}}$, then the entanglement entropy must scale as $S_A \approx an_A + bn_A^\gamma$ with $\gamma = \gamma_{\text{code}}$.
- (b) **Relation to black hole physics:** We will argue that a monitored quantum circuit can be interpreted as the Hayden-Preskill recovery problem, running backward in time, where the late Hawking radiations are sequentially measured projectively. This observation enables us to apply results from monitored quantum circuits to the problem of the black hole interior reconstruction.

2 Monitored quantum circuit as sequential measurements

We begin by formulating monitored quantum circuits in a generic form that can treat various cases on a unified footing.

Consider a system of n qubits. Initially the system is in a maximally mixed state $\mu \equiv \frac{I}{d}$ where $d = 2^n$ and I is an identity operator. A monitored quantum circuit implements a projective measurement of local Pauli operator P'_j and then time-evolves by a unitary operator U_j for $j = 1, \dots, \tau$. The circuit can be graphically represented as follows:



This setup can characterize various realizations of monitored quantum circuits. For instance, by taking $U_j = I$, one can account for the cases where multiple Pauli measurements are performed simultaneously. Also, if one hopes to study the cases where the initial states are product states instead of a maximally mixed state, one may measure all the n qubits with local Pauli operators at the beginning.

Instead of using local Pauli operators P'_j and time-evolution unitary operators U_j , it is convenient to consider time-evolved Pauli operators:

$$P_j \equiv (U_\tau \cdots U_j) P'_j (U_\tau \cdots U_j)^\dagger. \quad (5)$$

These time-evolved operators satisfy the following relation:

$$P_\tau \cdots P_1 = U_\tau P'_\tau U_{\tau-1} P'_{\tau-1} \cdots P'_2 U_1 P'_1 (U_\tau \cdots U_1)^\dagger. \quad (6)$$

Note that $(U_\tau \cdots U_1)^\dagger$ act trivially on the maximally mixed state μ . Hence, a monitored circuit can be formulated simply as sequential measurements of time-evolved Pauli operators P_j for $j = 1, \dots, \tau$. It is worth mentioning that this formulation can handle the measurement-only circuits [3] as well.

When a monitored circuit time-evolves by Clifford unitary operators, P_j are always Pauli operators (since the Clifford unitary operators transform Pauli operators into Pauli operators by its definition). Measurement projection operators are defined by

$$\Pi_j(m_j) \equiv \frac{I + m_j P_j}{2} \quad m_j = \pm 1 \quad (7)$$

where $m_j = \pm 1$ corresponds to the measurement outcomes. A monitored quantum circuit simply implements the following quantum operation

$$\Pi(m) \equiv \Pi_\tau(m_\tau) \cdots \Pi_1(m_1) \quad (8)$$

where m collectively denotes the measurement outcomes $m = (m_1, \dots, m_\tau)$. Namely, it can be expressed

as the following quantum channel:

$$\mathcal{Q}(\cdot) = \sum_m \Pi(m)(\cdot)\Pi^\dagger(m). \quad (9)$$

The probability of measuring m is given by

$$\text{Prob}(m) = \langle \Pi(m)^\dagger \Pi(m) \rangle = \frac{1}{d} \text{Tr} [\Pi(m)^\dagger \Pi(m)] \quad (10)$$

which can be graphically represented as follows:

$$\text{Prob}(m) = \begin{array}{c} \text{---} \bullet \text{---} \\ \boxed{\Pi_1^\dagger(m_1)} \\ \vdots \\ \boxed{\Pi_\tau^\dagger(m_\tau)} \\ \boxed{\Pi_\tau(m_\tau)} \\ \vdots \\ \boxed{\Pi_1(m_1)} \\ \text{---} \bullet \text{---} \end{array} \quad (11)$$

where each black dot represents a factor of $\frac{1}{\sqrt{d}}$.

In this paper, we are particularly interested in the entanglement structure of the output quantum state of a monitored quantum circuit. To be concrete, let us divide the Hilbert space into two subsystems A and B where A is a smaller subsystem. Here it is convenient to introduce a reference system R and purify the whole system. Then the output state of a monitored circuit is given by

$$|\Psi(m)\rangle = \frac{1}{\sqrt{\text{Prob}(m)}} \begin{array}{c} A \quad B \quad R \\ \boxed{\Pi_\tau(m_\tau)} \\ \vdots \\ \boxed{\Pi_2(m_2)} \\ \boxed{\Pi_1(m_1)} \\ \text{---} \bullet \text{---} \end{array} . \quad (12)$$

This expression is valid only when $\text{Prob}(m) \neq 0$. In the next several sections, we will develop a theoretical framework that enables us to study and verify the entanglement structure among subsystems A, B, R in monitored Clifford circuits.

3 Dual classical error-correction problem

In this section and the next two sections, we discuss the entanglement structure between two subsystems A and B . In this section, we will introduce a certain classical error-correction problem that is essential

in studying the entanglement structure of a monitored Clifford circuit.

3.1 Codeword and error vectors

We begin by introducing certain vectors which record commutation relations among Pauli operators P_A supported on the subsystem A and measured Pauli operators P_j in the past.

For Pauli operators $P_A \in \text{Pauli}_A$, we assign ± 1 using its commutation relations with respect to P_j as follows:

$$\mathcal{C}(P_A)_j = \pm 1 \quad P_A P_j = \pm P_j P_A \quad (j = 1, \dots, \tau). \quad (13)$$

We denote them collectively as vectors:

$$\mathcal{C}(P_A) = (\mathcal{C}(P_A)_1, \dots, \mathcal{C}(P_A)_\tau) \quad (14)$$

and call them *codeword vectors*.

As for P_i , we assign ± 1 according to its commutation relations with respect to other measured Pauli operators P_j as follows:

$$\begin{aligned} \mathcal{E}(P_i)_j &= 1 & (j > i) \\ \mathcal{E}(P_i)_j &= \pm 1 & P_i P_j = \pm P_j P_i \quad (j \leq i). \end{aligned} \quad (15)$$

Again we denote them collectively as vectors:

$$\mathcal{E}(P_i) = (\mathcal{E}(P_i)_1, \dots, \mathcal{E}(P_i)_\tau) \quad (16)$$

and call them *error vectors*. Here it is worth emphasizing that, if $i < j$, $\mathcal{E}(P_i)_j = 1$ regardless of the commutation relation between P_i and P_j . In other words, we will look at commutation relations with respect to operators in the past only, and not those in the future. So, the causal orderings of P_j are important.

Let us introduce a few more notations. We will consider the *error vector set* which is generated by component-wise multiplications of $\mathcal{E}(P_j)$ ³:

$$\mathcal{E} \equiv \left\langle \{ \mathcal{E}(P_j) \}_{\forall j} \right\rangle. \quad (19)$$

One can also define the following sets of vectors which are generated by acting error vectors $\mathcal{E}(P_i)$ on a

³In this paper, we mainly use “spin variables” instead of “binary variables” since spin variables are particularly useful in dealing with Pauli operators. For a spin variable $m_j = \pm 1$, we can associate the corresponding binary variables as follows:

$$m_j = \pm 1 \quad b(m_j) \equiv \frac{1 - m_j}{2} = 0, 1. \quad (17)$$

It is convenient to define “multiplications” and “summations” for these variables. Namely we have

$$m_i \cdot m_j \quad \leftrightarrow \quad b(m_i) + b(m_j) \quad (18)$$

where the summation is modulo 2.

codeword vector $\mathcal{C}(P_A)$:

$$\mathcal{E}^{(P_A)} \equiv \left\{ e \cdot \mathcal{C}(P_A) : e \in \mathcal{E} \right\}. \quad (20)$$

Note $\mathcal{E}^{(I_A)} = \mathcal{E}$. Finally it will be convenient to introduce the joint set of $\mathcal{E}^{(P_A)}$:

$$\mathcal{E}_{\text{total}} = \bigcup_{P_A \in \text{Pauli}_A} \mathcal{E}^{(P_A)}. \quad (21)$$

3.2 Classical error-correcting code

The above vectors $\mathcal{C}(P_A)$ and $\mathcal{E}(P_j)$ can be interpreted as codeword and error vectors in a classical error-correcting code.

To see this explicitly, assume that the subsystem A consists of n_A qubits. There are 4^{n_A} different Pauli operators on A , which can be viewed as $2n_A$ bits of classical information⁴. Let us think of encoding this $2n_A$ bits of classical information into τ physical bits. Here codewords are chosen according to commutation relations between a Pauli operator P_A on A and P_j 's:

$$P_A \in \text{Pauli}_A \xrightarrow{\text{encode}} \mathcal{C}(P_A) = (\mathcal{C}(P_A)_1, \dots, \mathcal{C}(P_A)_\tau). \quad (22)$$

This code attempts to encode $k = 2n_A$ logical bits into τ physical bits. In order for this code to be non-trivial, the encoding map $P_A \rightarrow \mathcal{C}(P_A)$ needs to be reversible (*i.e.* P_A needs to be encoded into a unique codeword $\mathcal{C}(P_A)$ for each P_A). In other words, P_A must have unique commutation relation profiles with respect to P_j .

Next, we discuss error vectors $\mathcal{E}(P_j)$. Imagine that vectors in \mathcal{E} act as possible errors on codeword vectors. To be concrete, assume that the initial codeword was $\mathcal{C}(P_A)$ and an error $e \in \mathcal{E}$ occurred. The resulting vector is $e \cdot \mathcal{C}(P_A)$:

$$\mathcal{C}(P_A) \xrightarrow{\text{error}} e \cdot \mathcal{C}(P_A) \quad e \in \mathcal{E}. \quad (23)$$

In order to recover the initial information, one must be able to reverse the action of error vectors:

$$e \cdot \mathcal{C}(P_A) \xrightarrow{\text{recovery?}} \mathcal{C}(P_A). \quad (24)$$

This will be possible when two codeword vectors are not connected by any error vector. Namely, in order for the initial information P_A to be fully recoverable, we must have

$$e \cdot \mathcal{C}(P_A) \neq f \cdot \mathcal{C}(Q_A) \quad \forall e, f \in \mathcal{E} \quad (P_A \neq Q_A). \quad (25)$$

Otherwise, two codewords $\mathcal{C}(P_A)$ and $\mathcal{C}(Q_A)$ cannot be reliably distinguished under the action of error vectors.

The above error-correction condition for full recovery can be rewritten in several equivalent ways as summarized below.

⁴For instance, when $n_A = 1$, we can assign $(1, 0)$ and $(0, 1)$ to Pauli X and Z operators respectively.

1) For all pairs of Pauli operators P_A, Q_A with $P_A \neq Q_A$, we must have

$$e \cdot \mathcal{C}(P_A) \neq \mathcal{C}(Q_A) \quad \forall e \in \mathcal{E}. \quad (26)$$

This follows from Eq. (25) by noting that $e \cdot f \in \mathcal{E}$ for $e, f \in \mathcal{E}$.

2) For all pairs of Pauli operators P_A, Q_A with $P_A \neq Q_A$, we must have

$$\mathcal{E}^{(P_A)} \cap \mathcal{E}^{(Q_A)} = \emptyset. \quad (27)$$

Here $\mathcal{E}^{(P_A)}$ can be interpreted as a set of all the vectors which $\mathcal{C}(P_A)$ may be transformed into by the action of error vectors. Hence, the joint set $\mathcal{E}_{\text{total}}$ must be divisible into 4^{n_A} distinct cosets $\mathcal{E}^{(P_A)}$ labelled by $P_A \in \text{Pauli}_A$.

3) All the non-identity Pauli operators $P_A (\neq I_A)$ must satisfy

$$\mathcal{E}^{(P_A)} \cap \mathcal{E}^{(I_A)} = \emptyset. \quad (28)$$

This follows from the previous condition 2) by noting that the encoding map is linear:

$$\mathcal{C}(P_A) \cdot \mathcal{C}(Q_A) = \mathcal{C}(P_A Q_A). \quad (29)$$

Such a classical code is called a linear code.

4) All the non-identity Pauli operators $P_A (\neq I_A)$ must satisfy

$$\mathcal{C}(P_A) \notin \mathcal{E}. \quad (30)$$

This follows from the previous condition 3). If this is not satisfied, the codeword $\mathcal{C}(P_A)$ would be indistinguishable from the codeword $\mathcal{C}(I_A)$ when acted by error vectors (since $\mathcal{E} = \mathcal{E}^{(I_A)}$).

We will mostly use the condition 4) in order to characterize the recoverability of the dual classical error-correcting code.

3.3 Entanglement structure from classical error-correction

By studying the dual classical error-correcting code, one can deduce the entanglement structure of a monitored Clifford circuit. Namely, recoverability of the initial information implies the presence of entanglement between A and B as summarized in the following theorem:

Theorem 1. *In a monitored Clifford circuit, a subsystem A is maximally entangled with its complement B with $I_{(A,B)} = 2n_A$ if and only if the initial information in the dual classical error-correcting code is fully recoverable.*

It is worth emphasizing that the theorem applies to arbitrary realizations of measurement outcomes $m = (m_1, \dots, m_\tau)$.

When the classical error-correction condition is not satisfied, two subsystems A and B are not maximally entangled. In these cases, we can still compute a certain entanglement measure between A

and B . Here, we will focus on the conditional entropy of A given B :

$$S_{A|B} \equiv S_{AB} - S_B. \quad (31)$$

Recall that the conditional entropy is positive in classical systems, but can be negative in quantum systems. Namely, it is useful to note

$$S_{A|B} = S_R - S_{AR} \geq -S_A \quad (32)$$

where we used the fact that the output quantum state of the monitored circuit is pure on ABR in the first equality. The second inequality used the positivity of the mutual information $I_{(A,R)} \equiv S_A + S_R - S_{AR} \geq 0$. The equality is achieved when A and R are not correlated at all with $I_{(A,R)} = 0$. The minimal value of the conditional entropy is $-n_A$, and it is achieved when A and B are maximally entangled with $I_{(A,B)} = 2n_A$.

When we interpret the outcome $|\Psi(m)\rangle$ as a quantum channel from A to B , the conditional entropy $S_{A|B}$ can be viewed as the coherent quantum information of the quantum channel. So, $S_{A|B}$ characterizes how much quantum information can be transmitted from A to B when viewed as a quantum channel.

Let us denote the value of the conditional entropy for the measurement result of $m = (m_1, \dots, m_\tau)$ by $S_{A|B}(m)$. We will prove the following theorem.

Theorem 2. *The conditional entropy is given by*

$$S_{A|B}(m) = -n_A + \log_2 N_{I_A} \quad (33)$$

where N_{I_A} is the number of $P_A \in \text{Pauli}_A$ such that $\mathcal{C}(P_A) \in \mathcal{E}^{(I_A)}$.

Note that theorem 1 follows from theorem 2.

The proof of this theorem will be presented in appendix C. When the classical error-correction condition is satisfied, we have $N_{I_A} = 1$ and $S_{A|B}(m) = -n_A$. Then, from Eq. (32), we find that $S_A = n_A$ and thus, $I_{(A,B)} = S_A + S_B - S_{AB} = 2n_A$. Hence, A and B are maximally entangled. It is worth emphasizing that $S_{A|B}(m)$ does not depend on measurement outcomes $m = (m_1, \dots, m_\tau)$. Here it is useful to observe that N_{I_A} can be interpreted as the number of lost classical information since P_A becomes indistinguishable from I_A .

Later we will discuss why the conditional entropy $S_{A|B}$, instead of the mutual information $I_{(A,B)}$, can be computed in the framework of using the dual classical error-correcting code.

3.4 Examples

Since codeword vectors and error vectors play particularly important roles in the entanglement structure of a Clifford monitored circuit, it is worth looking at several examples.

3.4.1 Commuting P_j 's

Let us begin by looking at the case where $[P_i, P_j] = 0$. Assume that $n = 3$. Assume that A is the first qubit, and B consists of the second and the third qubits. So, we have

$$\begin{aligned} I_A &= I_1 \otimes I_2 \otimes I_3 \\ X_A &= X_1 \otimes I_2 \otimes I_3 \\ Y_A &= Y_1 \otimes I_2 \otimes I_3 \\ Z_A &= Z_1 \otimes I_2 \otimes I_3. \end{aligned} \tag{34}$$

Let us choose P_1, P_2, P_3 as follows:

$$\begin{aligned} P_1 &= X_1 \otimes X_2 \otimes I_3 \\ P_2 &= Z_1 \otimes Z_2 \otimes X_3 \\ P_3 &= Y_1 \otimes Z_2 \otimes Z_3. \end{aligned} \tag{35}$$

One can check that P_j 's commute with each other.

In this monitored circuit, the system starts from the maximally mixed state $\mu = \frac{I}{2^3}$, and then measurements of P_1, P_2, P_3 are performed sequentially. We are interested in whether the subsystem A is entangled with its complement B or not.

We can construct the codeword vectors and error vectors as follows:

	P_1	P_2	P_3
$\mathcal{C}(I_A)$	1	1	1
$\mathcal{C}(X_A)$	1	-1	-1
$\mathcal{C}(Y_A)$	-1	-1	1
$\mathcal{C}(Z_A)$	-1	1	-1
$\mathcal{E}(P_1)$	1	1	1
$\mathcal{E}(P_2)$	1	1	1
$\mathcal{E}(P_3)$	1	1	1

We see that all the error vectors are trivial; $(1, 1, 1)$. Hence the error vector set is given by

$$\mathcal{E} = \{(1, 1, 1)\}. \tag{36}$$

Also, observe that codeword vectors are unique. Hence, we have

$$\begin{aligned} \mathcal{E}^{(I_A)} &= \{(1, 1, 1)\} \\ \mathcal{E}^{(X_A)} &= \{(1, -1, -1)\} \\ \mathcal{E}^{(Y_A)} &= \{(-1, -1, 1)\} \\ \mathcal{E}^{(Z_A)} &= \{(-1, 1, -1)\} \end{aligned} \tag{37}$$

which do not overlap with each other. We saw that P_A is encoded into the codewords $\mathcal{C}(P_A)$ in a unique manner, and the error from \mathcal{E} cannot connect different codewords. Hence the initial information about P_A is recoverable, which implies that A is maximally entangled with B .

As this example suggests, when $[P_i, P_j] = 0$ for all i, j , A and B are maximally entangled if and only if the codewords $\mathcal{C}(P_A)$ are unique for different P_A . This was originally pointed out [25] in the context

of the Hayden-Preskill recovery problem.

3.4.2 Non-commuting P_j 's (recoverable)

Next, let us choose P_1, P_2, P_3 as follows:

$$\begin{aligned} P_1 &= X_1 \otimes Z_2 \otimes I_3 \\ P_2 &= Z_1 \otimes I_2 \otimes X_3 \\ P_3 &= I_1 \otimes X_2 \otimes X_3. \end{aligned} \tag{38}$$

Codeword vectors and error vectors are given as follows:

	P_1	P_2	P_3
$\mathcal{C}(I_A)$	1	1	1
$\mathcal{C}(X_A)$	1	-1	1
$\mathcal{C}(Y_A)$	-1	-1	1
$\mathcal{C}(Z_A)$	-1	1	1
$\mathcal{E}(P_1)$	1	1	1
$\mathcal{E}(P_2)$	-1	1	1
$\mathcal{E}(P_3)$	-1	1	1

The error vector set is given by

$$\mathcal{E} = \{(1, 1, 1), (1, -1, -1)\}. \tag{39}$$

We also have

$$\begin{aligned} \mathcal{E}^{(I_A)} &= \{(1, 1, 1), (1, -1, -1)\} \\ \mathcal{E}^{(X_A)} &= \{(1, -1, 1), (1, 1, -1)\} \\ \mathcal{E}^{(Y_A)} &= \{(-1, -1, 1), (-1, 1, -1)\} \\ \mathcal{E}^{(Z_A)} &= \{(-1, 1, 1), (-1, -1, -1)\} \end{aligned} \tag{40}$$

which do not overlap with each other. Hence, the codewords $\mathcal{C}(P_A)$ are recoverable under the errors from \mathcal{E} . In this case, A is maximally entangled with B .

3.4.3 Non-commuting P_j 's (not recoverable)

Let us choose P_1, P_2, P_3 as follows:

$$\begin{aligned} P_1 &= X_1 \otimes I_2 \otimes Z_3 \\ P_2 &= Z_1 \otimes Z_2 \otimes Z_3 \\ P_3 &= Y_1 \otimes Z_2 \otimes Z_3. \end{aligned} \tag{41}$$

We then have

	P_1	P_2	P_3
$\mathcal{C}(I_A)$	1	1	1
$\mathcal{C}(X_A)$	1	-1	-1
$\mathcal{C}(Y_A)$	-1	-1	1
$\mathcal{C}(Z_A)$	-1	1	-1
$\mathcal{E}(P_1)$	1	1	1
$\mathcal{E}(P_2)$	-1	1	1
$\mathcal{E}(P_3)$	-1	-1	1

The error vector set is given by

$$\mathcal{E} = \{(1, 1, 1), (-1, 1, 1), (-1, -1, 1), (1, -1, 1)\}. \quad (42)$$

We also have

$$\begin{aligned} \mathcal{E}^{(I_A)} &= \{(1, 1, 1), (-1, 1, 1), (-1, -1, 1), (1, -1, 1)\} \\ \mathcal{E}^{(X_A)} &= \{(1, -1, -1), (-1, -1, -1), (-1, 1, -1), (1, 1, -1)\} \\ \mathcal{E}^{(Y_A)} &= \{(-1, -1, 1), (1, -1, 1), (1, 1, 1), (-1, 1, 1)\} \\ \mathcal{E}^{(Z_A)} &= \{(-1, 1, -1), (1, 1, -1), (1, -1, -1), (-1, -1, -1)\} \end{aligned} \quad (43)$$

which are not distinct. Hence, the codewords $\mathcal{C}(P_A)$ are not recoverable under the errors from \mathcal{E} . In this case, A is not maximally entangled with B . Namely, we will have $S_{A|B} = 0$.

4 Entanglement distillation between two subsystems

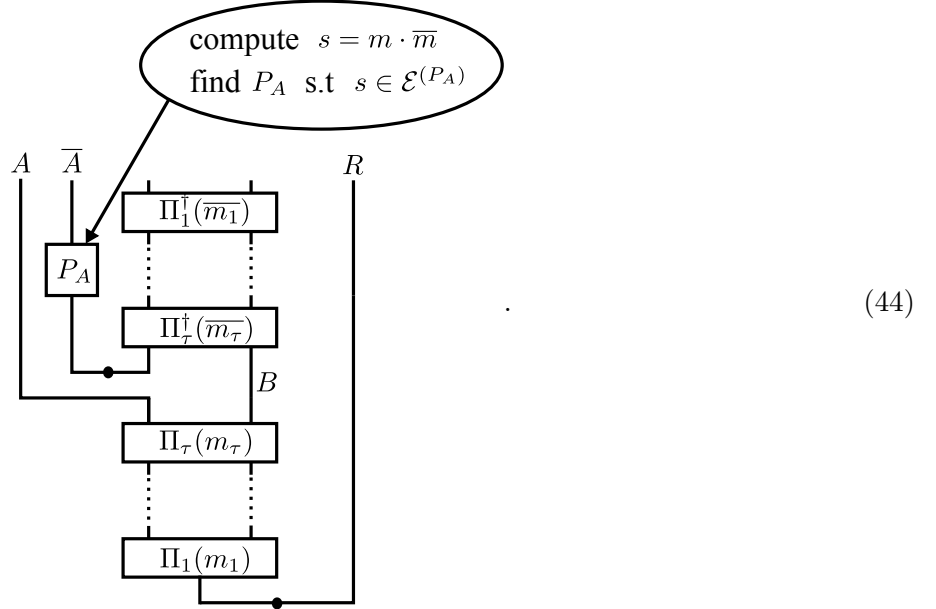
In this section, we will describe the entanglement distillation algorithm and compute its output.

4.1 Perfect distillation

To build some intuition, we begin by discussing the cases where A and B are maximally entangled (*i.e.* the classical error-correction condition is satisfied).

The distillation algorithm proceeds in a way similar to algorithms from [17, 25, 26]. The overall

procedure is graphically summarized as follows:



Given the outcome of the monitored circuit $|\Psi(m)\rangle$, we keep qubits on A aside and add EPR pairs on $A\bar{A}$. Then we perform projective measurements of $P_\tau^\dagger, \dots, P_1^\dagger$ whose measurement outcomes are denoted by \bar{m} . This process can be written as $\Pi(\bar{m})^\dagger$. Finally, some appropriate feedback operation is applied on \bar{A} based on the measurement results m and \bar{m} .

Let us discuss how to construct an appropriate feedback operator. It is convenient to define a sum vector s via component-wise multiplications:

$$s \equiv m \cdot \bar{m}. \quad (45)$$

We will prove that the measurement of m and \bar{m} may occur only when $s = m \cdot \bar{m} \in \mathcal{E}_{\text{total}}$ where $\mathcal{E}_{\text{total}} = \bigcup_{P_A} \mathcal{E}^{(P_A)}$. In fact, we can compute the probability of measuring s explicitly. Let us denote the probability of measuring m and \bar{m} by $\text{Prob}(m, \bar{m})$. It is convenient to define the summation of probabilities over m as follows:

$$\text{Sum}(s) \equiv \sum_m \text{Prob}(m, m \cdot s) \quad (46)$$

which corresponds to the total probability of measuring s . We will prove the following lemma.

Lemma 1. *The probability of measuring s is given by*

$$\begin{aligned} \text{Sum}(s) &\equiv \sum_m \text{Prob}(m, m \cdot s) = \frac{1}{d_{\mathcal{E}_{\text{total}}}} & s \in \mathcal{E}_{\text{total}} \\ &= 0 & s \notin \mathcal{E}_{\text{total}} \end{aligned} \quad (47)$$

where $d_{\mathcal{E}_{\text{total}}}$ is the number of elements in the joint set $\mathcal{E}_{\text{total}}$.

So, measurement of s with $s \notin \mathcal{E}_{\text{total}}$ will never occur. The proof of this lemma will be presented in appendix A.

Now we discuss how to construct a feedback operator. One immediate corollary of lemma 1 is that one can always find $P_A \in \text{Pauli}_A$ such that

$$s \in \mathcal{E}^{(P_A)}. \quad (48)$$

It turns out that the necessary feedback operation is to simply implement P_A on \bar{A} . In general, there can be multiple P_A which satisfy $s \in \mathcal{E}^{(P_A)}$. But, when the classical error-correction condition is satisfied, then one can always find a unique P_A satisfying $s \in \mathcal{E}^{(P_A)}$. Hence, the task of finding P_A can be interpreted as decoding of the initial classical information P_A from a bit string s in the dual classical code.

One comment follows. When the measurement result satisfies $s \in \mathcal{E} = \mathcal{E}^{(I_A)}$, there is no need of applying a feedback operation. If the classical error-correction condition is satisfied, this occurs with the following probability

$$\frac{\sum_{s \in \mathcal{E}^{(I_A)}} \text{Sum}(s)}{\sum_{s \in \mathcal{E}_{\text{total}}} \text{Sum}(s)} = \frac{1}{d_A^2}. \quad (49)$$

This probability matches with the successful post-selection decoding probability for the Hayden-Preskill decoding algorithm [17].

Here we summarize the distillation algorithm.

1. Given the outcome of the monitored circuit $|\Psi(m)\rangle$, keep qubits on A aside and insert ancilla EPR pairs on \bar{A} and A .
2. Perform measurements of $P_\tau^\dagger, \dots, P_1^\dagger$ by applying $\Pi^\dagger(\bar{m})$.
3. Compute $s = m \cdot \bar{m}$ and find $P_A \in \text{Pauli}_A$ such that $s \in \mathcal{E}^{(P_A)}$.
4. Apply P_A on \bar{A} . Perfect EPR pairs will be distilled on A and \bar{A} if the classical error-correction condition is satisfied.

4.2 Imperfect distillation

If the recoverability condition is not satisfied, the outcome of the distillation algorithm will prepare imperfect EPR pairs. Here we will explicitly compute the output state, averaged over all the possible measurement results m, \bar{m} .

Let us denote the output of the aforementioned distillation algorithm by $\sigma_{A\bar{A}}(m, \bar{m})$. We are particularly interested in its statistical average defined by

$$\mathbb{E}(\sigma_{A\bar{A}}) \equiv \sum_{m, \bar{m}} \text{Prob}(m, \bar{m}) \sigma_{A\bar{A}}(m, \bar{m}). \quad (50)$$

The averaged output quantum state can be computed explicitly as follows:

Lemma 2. *The output of the aforementioned distillation algorithm for a monitored Clifford circuit is*

$$\mathbb{E}(\sigma_{A\bar{A}}) = \frac{1}{N_{I_A}} \sum_{P_A: \mathcal{C}(P_A) = \mathcal{E}^{(I_A)}} |P_A\rangle\langle P_A| \quad (51)$$

where N_{I_A} is the number of P_A such that $\mathcal{C}(P_A) = \mathcal{E}^{(I_A)}$.

Here, $|P_A\rangle$ represents the Choi-Jamiołkowski state of P_A , namely

$$|P_A\rangle \equiv (P_A \otimes I_{\bar{A}})|\text{EPR}\rangle_{A\bar{A}}. \quad (52)$$

Note that $|P_A\rangle$'s form a complete orthonormal basis for A and \bar{A} . The proof of this lemma will be presented in appendix B.

The statistical average $\mathbb{E}(\sigma_{A\bar{A}})$ can capture quantum entanglement between A and B even though it is averaged over all the possible realizations of m and \bar{m} . Let us compute the conditional entropy $S_{A|\bar{A}}$ for $\mathbb{E}(\sigma_{A\bar{A}})$:

$$S_{A|\bar{A}} \text{ of } \mathbb{E}(\sigma_{A\bar{A}}) = \log N_{I_A} - n_A \quad (53)$$

which matches with the value from theorem 2:

$$S_{A|B}(m) = \log N_{I_A} - n_A. \quad (54)$$

4.3 Examples

It will be useful to look at concrete examples in order to gain some intuitions. For simplicity of discussion, we will focus on systems with two qubits ($n = 2$) with $n_A = n_B = 1$.

4.3.1 No measurement

Let us begin with the most trivial case. If no measurement is performed at all, the output is

$$\mu_A \otimes \mu_B \quad (55)$$

where μ_A and μ_B are maximally mixed states on A and B respectively. The conditional entropy is

$$S_{A|B} = 1. \quad (56)$$

4.3.2 Single-qubit measurement

Assume that there was only a single measurement with $\tau = 1$, and it was with $P_1 = Z_A$. In this case, the output of the monitored circuit is

$$\begin{aligned} |0\rangle\langle 0|_A \otimes \mu_B & \quad m_1 = 1 \\ |1\rangle\langle 1|_A \otimes \mu_B & \quad m_1 = -1. \end{aligned} \quad (57)$$

One can see that A and B have no correlation at all. For both cases, we have

$$S_{A|B}(m_1) = 0 \quad m_1 = \pm 1. \quad (58)$$

The output for the entanglement distillation algorithm is

$$\begin{aligned} |0\rangle\langle 0|_A \otimes |0\rangle\langle 0|_{\bar{A}} & \quad m_1 = 1 \\ |1\rangle\langle 1|_A \otimes |1\rangle\langle 1|_{\bar{A}} & \quad m_1 = -1. \end{aligned} \quad (59)$$

Hence its average over m_1 is given by

$$\mathbb{E}(\rho_{A|\bar{A}}) = \frac{1}{2}(|00\rangle\langle 00| + |11\rangle\langle 11|) \quad (60)$$

which possesses classical correlation. Note that this classical correlation was generated by taking an average over m_1 . Finally we can see that the conditional entropy is given by

$$S_{A|\bar{A}} \text{ of } \mathbb{E}(\sigma_{A|\bar{A}}) = 0. \quad (61)$$

It is worth computing the mutual information. For the output of a monitored circuit, we have

$$I_{(A,B)}(m_1) = 0 \quad m_1 = \pm 1 \quad (62)$$

where $I_{(A,B)} \equiv S_A + S_B - S_{AB}$. On the other hand, for the averaged output of the distillation algorithm, we have

$$I_{(A,\bar{A})} \text{ of } \mathbb{E}(\sigma_{A|\bar{A}}) = 1 \quad (63)$$

due to the classical correlation. Hence, the values of the mutual information do not match.

4.3.3 Two-qubit measurement

Next, assume that there was only a single measurement with $\tau = 1$, and it was with $P_1 = Z_A \otimes Z_B$. In this case, the output of the monitored circuit is

$$\begin{aligned} \frac{1}{2}(|00\rangle\langle 00| + |11\rangle\langle 11|) & \quad m_1 = 1 \\ \frac{1}{2}(|01\rangle\langle 01| + |10\rangle\langle 10|) & \quad m_1 = -1. \end{aligned} \quad (64)$$

One can see that A and B share classical correlation which was induced by measurement of $Z_A \otimes Z_B$. We find

$$S_{A|B}(m_1) = 0 \quad m_1 = \pm 1. \quad (65)$$

The output for the entanglement distillation algorithm is

$$\frac{1}{2}(|00\rangle\langle 00| + |11\rangle\langle 11|) \quad m_1 = \pm 1. \quad (66)$$

Note that classical correlation is present even without taking an average over m_1 . We see that the conditional entropy is given by

$$S_{A|\bar{A}} \text{ of } \mathbb{E}(\sigma_{A|\bar{A}}) = 0. \quad (67)$$

As for the mutual information, we have

$$I_{(A,B)}(m_1) = 1 \quad m_1 = \pm 1 \quad (68)$$

and

$$I_{(A,\bar{A})} \text{ of } \mathbb{E}(\sigma_{A|\bar{A}}) = 1. \quad (69)$$

Hence, the values of the mutual information match.

One important lesson from this and previous examples is that the monitored quantum circuits generate different output states in two examples, but the averaged output $\mathbb{E}(\sigma_{A\bar{A}})$ from the distillation algorithm is the same for both cases. This is because $Z_A \otimes I_B$ and $Z_A \otimes Z_B$ have the same patterns of commutation relations with P_A . This is also the reason why the conditional entropy, instead of the mutual information, is computable from the dual classical code.

4.3.4 Two-qubit commuting measurement

Next, assume that we perform two commuting measurements with $P_1 = X_A \otimes X_B$ and $P_2 = Z_A \otimes Z_B$. In this case, the output of the monitored circuit is

$$|I_A\rangle, |X_A\rangle, |Y_A\rangle, |Z_A\rangle \quad (m_1, m_2) = (1, 1), (1, -1), (-1, -1), (-1, 1) \quad (70)$$

where $|P_A\rangle \equiv (P_A \otimes I_B)|\text{EPR}\rangle_{AB}$. All the possible output states are maximally entangled, and we have

$$S_{A|B}(m_1, m_2) = -1 \quad m_1, m_2 = \pm 1. \quad (71)$$

The outputs for the entanglement distillation algorithm are

$$|I_A\rangle = |\text{EPR}\rangle_{AB} \quad m_1, m_2 = \pm 1 \quad (72)$$

and the conditional entropy is given by

$$S_{A|\bar{A}} \text{ of } \mathbb{E}(\sigma_{A|\bar{A}}) = -1. \quad (73)$$

In this case, the codeword vectors are

$$\mathcal{C}(I_A) = (1, 1) \quad \mathcal{C}(X_A) = (1, -1) \quad \mathcal{C}(Y_A) = (-1, -1) \quad \mathcal{C}(Z_A) = (-1, 1). \quad (74)$$

Also, the error vector set is trivial $\mathcal{E} = \{(1, 1)\}$ because P_1 and P_2 commute. Hence, the classical error-correction condition is satisfied.

4.3.5 Two-qubit non-commuting measurement

Finally, assume that we perform two on-commuting measurements with $P_1 = X_A \otimes Z_B$ and $P_2 = Z_A \otimes Z_B$. In this case, the output of the monitored circuit is

$$\begin{aligned} \frac{1}{2}(|00\rangle\langle 00| + |11\rangle\langle 11|) & \quad m_1 = \pm 1, \quad m_2 = 1 \\ \frac{1}{2}(|01\rangle\langle 01| + |10\rangle\langle 10|) & \quad m_1 = \pm 1, \quad m_2 = -1. \end{aligned} \quad (75)$$

Note that the measurement result m_1 does not affect the output state. The outputs for the entanglement distillation algorithm is

$$\frac{1}{2}(|00\rangle\langle 00| + |11\rangle\langle 11|) \quad m_1 = \pm 1, \quad m_2 = \pm 1. \quad (76)$$

We see that the two subsystems share classical correlations only.

In this case, the codeword vectors are

$$\mathcal{C}(I_A) = (1, 1) \quad \mathcal{C}(X_A) = (1, -1) \quad \mathcal{C}(Y_A) = (-1, -1) \quad \mathcal{C}(Z_A) = (-1, 1). \quad (77)$$

The error vector set is trivial $\mathcal{E} = \{(1, 1), (-1, 1)\}$ because P_1 and P_2 anti-commute. Hence, the classical error-correction condition is not satisfied. We have

$$\mathcal{E}^{(I_A)} = \mathcal{E}^{(Z_A)} = \{(1, 1), (-1, 1)\} \quad \mathcal{E}^{(X_A)} = \mathcal{E}^{(Y_A)} = \{(1, -1), (-1, -1)\} \quad (78)$$

which suggests that the output of the distillation algorithm is

$$\frac{1}{2}(|I_A\rangle\langle I_A| + |Z_A\rangle\langle Z_A|) = \frac{1}{2}(|00\rangle\langle 00| + |11\rangle\langle 11|). \quad (79)$$

4.4 Distillation algorithm for the Gullans-Huse proposal

Let us apply the aforementioned distillation algorithm to the proposal by Gullans and Huse which entangles the system to a single reference qubit [20].

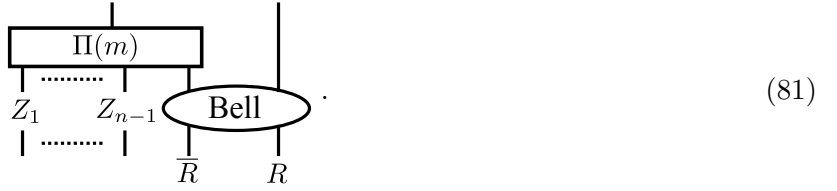
Consider an EPR pair on $R\bar{R}$ where each of R and \bar{R} consists of a single qubit. Here we think of encoding \bar{R} into n qubits by some Clifford isometry and use it as an initial state of the monitored Clifford circuit. One can represent the output wavefunction as follows:


(80)

by adding $n - 1$ ancilla qubits prepares in $|0\rangle^{\otimes n-1}$. Here the encoding circuit is absorbed into the definition of measured Pauli operators P_j . The key idea of the Gullans-Huse proposal is that the entanglement between the system and the reference will survive for long time when the monitored quantum circuit is in the volume-law phase. Hence, the distillability of an EPR pair serves as an order parameter to detect the dynamical entanglement phase transition. Our goal is to construct an algorithm to distill an EPR pair from the system and the reference in this setup.

The aforementioned algorithm was designed to distill the entanglement within the system. In order to apply it to the Gullans-Huse proposal, we will view the whole of $n+1$ qubits (including the reference R) as the “system” of the monitored Clifford circuit. Namely, we imagine that the system was initially in the maximally mixed state, and then we performed measurements of Z_1, \dots, Z_{n-1} and Bell measurements

$X_n \otimes X_{n+1}$ and $Z_n \otimes Z_{n+1}$:



Eq. (80) can be obtained by postselecting the measurement outcomes to $Z_j = +1$ and $X_n \otimes X_{n+1} = Z_n \otimes Z_{n+1} = +1$. In this interpretation, we need to extend codeword vectors and error vectors as follows

$$\mathcal{C}(P_R) = (\text{Bell}, Z_j\text{'s}, P_j\text{'s}) \quad (82)$$

so that commutation relations with Bell operators and Z_j 's at the beginning are taken into account. The distillation algorithm is given by



where measurements of Z_j 's and Bell operators are performed at the very end of the algorithm. The Bell measurements at the very end can be omitted, leading to the following simplified algorithm:



This simplification has an effect of restricting the sum vector s to be $s = (+1, Z_j\text{'s}, P_j\text{'s})$. By decoding this sum vector, one can obtain an appropriate feedback Pauli operator P_R to distill an EPR pair on $R\bar{R}$ (if the system and the reference remain entangled).

5 Operator growth in spacetime

Previous works have noted that the scrambling dynamics in a monitored quantum circuit underpins the emergence of the volume-law entanglement. While this speculation would have profound implications, concrete arguments establishing this connection have not been presented. Indeed, entanglement creation in unitary quantum circuits is a process of thermalization that has no direct relevance to quantum information scrambling⁵. Namely, unlike thermalization which concerns the time-evolution of a

⁵This confusion can be found in earlier works on the fast scrambling conjecture, see [27] for instance. Recent studies have found that entanglement creation may not occur in the scrambling time scale [28]. A related observation can be found

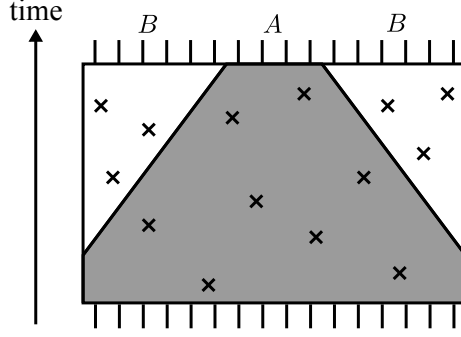


Figure 3: Operator growth and entanglement creation in a monitored quantum circuit. Cross marks represent measured Pauli operators. A local Pauli operator P_A on A is encoded into a codeword vector by overlapping with measured Pauli operators in the past which lie inside the shaded region of the spacetime.

quantum state, quantum information scrambling stems from the growth of local operators which can be quantitatively measured by using out-of-time order correlation (OTOC) functions [29–31].

Our characterization establishes a direct and concrete relation between entanglement in monitored quantum circuits and the operator growth. A central object in our analysis was the codeword vector $\mathcal{C}(P_A)$ which can be understood as OTOC functions:

$$\mathcal{C}(P_A)_j = \langle P_A P_j P_A^\dagger P_j^\dagger \rangle. \quad (85)$$

For the subsystem A to be entangled with B , the underlying dynamic (the unitary part of the monitored circuit) needs to be scrambling. Namely, P_A should evolve back and overlap non-trivially with measured Pauli operators P_j in the past so that the codeword vector $\mathcal{C}(P_A)$ is non-trivial and resilient against errors (see Fig. 3). A crucial point is that, without local P_j measurements, the subsystem A would be entangled with the reference R . Local projective measurements P_j decouple A from the reference R , and instead make A entangled with its complement B .

Here, it is important to emphasize that entanglement creation in the volume-law phase is a result of a subtle competition between the decoupling phenomena and accumulations of error vectors in \mathcal{E} . Namely, while overlapping with operators in the past is crucial for robust codeword vectors $\mathcal{C}(P_A)$, too many projective measurements will make the error vector set \mathcal{E} rather dense and bring the system to the area-law phase. Also, our analyses in this paper so far primarily focus on Clifford circuits. It is worth noting, however, that the decoupling phenomena, which disentangles A from R , is a generic feature of scrambling systems, and is not restricted to Clifford circuits [32]. We expect that the space-time pattern of the operator growth will be an interesting subject of study, and hope to further establish the connection between scrambling dynamics and entanglement creation in monitored quantum circuits beyond Clifford in a future work.

6 Coding properties of monitored Clifford circuit

So far, we have studied the entanglement between two complementary subsystems without involving the reference system. In this section and the next, we turn our attentions to the entanglement structure of

in [29] as well.

monitored Clifford circuits with the reference system R . In this section, we study the coding properties of monitored Clifford circuits. Some additional results are presented in appendix E as well.

6.1 System-Reference entanglement

Our framework of using a dual classical error-correcting code allows us to study the entanglement structure among subsystems A, B as well as the reference system R .

Recall that we used Pauli operators $P_A \in \text{Pauli}_A$ on a subsystem A as initial information of a classical error-correcting code and derived the conditional entropy $S_{A|B}$:

$$S_{A|B} = S_{AB} - S_B = \log N_{I_A} - n_A \quad N_{I_A} : \text{number of } P_A \text{ s.t. } \mathcal{C}(P_A) \in \mathcal{E}. \quad (86)$$

One can repeat a similar analysis by choosing $P_B \in \text{Pauli}_B$ on a subsystem B as initial information:

$$S_{A|B} = S_{AB} - S_A = \log N_{I_B} - n_B \quad N_{I_B} : \text{number of } P_B \text{ s.t. } \mathcal{C}(P_B) \in \mathcal{E}. \quad (87)$$

One can also use all the Pauli operators P supported on AB and treat them as initial information. This leads to

$$S_{AB|\emptyset} = S_{AB} = \log N_I - n \quad N_I : \text{number of } P \text{ s.t. } \mathcal{C}(P) \in \mathcal{E}. \quad (88)$$

Here we interpreted AB as a system of interest so that AB 's complement is an empty set \emptyset .

These three equations Eq. (86) (87) (88) are sufficient to specify values of entanglement entropies for all the possible subsystems, namely $(S_A, S_B, S_R, S_{AB}, S_{BR}, S_{AR})$. Here we compute a few interesting entanglement measures. Let us begin with the mutual information $I_{(A,B)}$:

$$I_{(A,B)} = \log \frac{N_I}{N_{I_A} N_{I_B}} \quad (89)$$

which can be expressed in terms of the numbers of Pauli operators such that $\mathcal{C}(P) \in \mathcal{E}$. Namely there may exist a Pauli operator $P = P_A \otimes P_B$ such that $\mathcal{C}(P_A), \mathcal{C}(P_B) \notin \mathcal{E}$, but $\mathcal{C}(P) \in \mathcal{E}$. The above equation suggests that $I_{(A,B)}$ is related to the number of such Pauli operators which are non-local with respect to the bipartition into A and B .

Next, let us compute the conditional entropy $S_{AB|R}$:

$$S_{AB|R} = n - \log N_I \quad (90)$$

where we used $S_{ABR} = 0$. One also finds $I_{(AB,R)} = 2(\log N_I - n)$. Observe that N_I is related to the amount of lost information in the dual classical error-correcting code since a Pauli operator P is indistinguishable from an identity operator I . It is interesting to note that the entanglement between the system A and the reference R results from the loss of initial information in the dual classical error-correcting code. Intuitively, this result suggests that the lost information, which was not detected by P_j 's, will flow to the reference R .

As is evident from discussions so far, Pauli operators satisfying P with $\mathcal{C}(P) \in \mathcal{E}$, which is indistinguishable from I , play important roles in studying the entanglement structure of a monitored Clifford circuit. We shall call them *null operators* of a dual classical error-correcting code. For later discussions,

it will be convenient to define the following three sets of null operators:

$$\begin{aligned}\mathcal{L} &\equiv \{P \in \text{Pauli} : \mathcal{C}(P) \in \mathcal{E}\} \\ \mathcal{L}_A &\equiv \{P_A \in \text{Pauli}_A : \mathcal{C}(P_A) \in \mathcal{E}\} \\ \mathcal{L}_B &\equiv \{P_B \in \text{Pauli}_B : \mathcal{C}(P_B) \in \mathcal{E}\}.\end{aligned}\tag{91}$$

Note that these sets are actually groups⁶. Later, we will show that these null operators serve as logical operators (including trivial stabilizer operators) when the monitored Clifford circuit is viewed as a quantum error-correcting code.

6.2 Stabilizer group

In this subsection and the next, we will construct stabilizer and logical operators of a monitored Clifford circuit. We begin by constructing the stabilizer group \mathcal{S} . The construction proceeds recursively. Here we denote the stabilizer group constructed for P_t, \dots, P_1 by $\text{Stab}^{(t)}$. We start with

$$\text{Stab}^{(1)} \equiv \langle P_1 \rangle\tag{92}$$

and then recursively define

$$\text{Stab}^{(\tau)} \equiv \langle P_\tau, \{P \in \text{Stab}^{(\tau-1)} : [P, P_\tau] = 0\} \rangle.\tag{93}$$

It is worth emphasizing that this is different from simply taking the center of the group $\langle \{P_j\} \rangle$.

To gain some insight on this construction, let us make the following observations. If P_τ commutes with all the Pauli operators in $\text{Stab}^{(\tau-1)}$, we have

$$\text{Stab}^{(\tau)} = \langle P_\tau, \text{Stab}^{(\tau-1)} \rangle.\tag{94}$$

On the other hand, if there exists $R \in \text{Stab}^{(\tau-1)}$ such that $\{R, P_\tau\} = 0$, R is removed and then P_τ will be added to the stabilizer group. In other words, all the Pauli operators which do not commute with P_τ are removed, and instead, P_τ is added to the group. It is useful to note

$$P_\tau \in \text{Stab}^{(\tau)} \quad \text{and} \quad [Q, P_\tau] = 0 \quad \forall Q \in \text{Stab}^{(\tau)}.\tag{95}$$

So, the last Pauli operator P_τ always enter in the latest stabilizer group $\text{Stab}^{(\tau)}$.

Let us briefly discuss the physical implication of the recursive construction of $\text{Stab}^{(\tau)}$. Observe that the number of operators in $\text{Stab}^{(\tau)}$ increases if and only if P_τ commutes with all the operators in $\text{Stab}^{(\tau-1)}$, and is not included in $\text{Stab}^{(\tau-1)}$. In general, this is not very likely to occur when $\text{Stab}^{(\tau-1)}$ is already large. Namely, if $\dim \text{Stab}^{(\tau-1)} = 2^{n_S}$ and P_τ is randomly chosen, the increase will occur only with probability $\approx \frac{1}{2^{n_S}}$. Here it is natural to expect that P_τ is a high-weight pseudorandom Pauli operator when the underlying dynamics is scrambling. Hence, the size of $\text{Stab}^{(\tau)}$ will not increase easily once the circuit reaches the entanglement equilibrium. This mechanism is crucial in an exponential memory time in the volume-law phase of monitored quantum circuits.

The constructed group $\mathcal{S} \equiv \text{Stab}^{(\tau)}$ plays the role of the stabilizer group. Given the aforementioned

⁶Strictly speaking, a complex phase iI should be included to define a group of Pauli operators. We ignore this subtlety since it is not essential in our treatment. For careful analyses, see [33, 34] for instance.

construction, the following lemma can be proven immediately.

Lemma 3. *Let $P \in \mathcal{S}$ be a Pauli operator in the stabilizer group \mathcal{S} of the monitored Clifford circuit. Then we have*

$$P|\Psi(m)\rangle = \pm|\Psi(m)\rangle \quad (96)$$

where the eigenvalue ± 1 depends on the measurement outcome m .

In a conventional stabilizer code, stabilizer generators S_j are chosen so that codeword states are supported on a subspace satisfying $S_j|\psi\rangle = +|\psi\rangle$. In a monitored Clifford circuit, the signs of eigenvalues with respect to stabilizer generators depend on the measurement outcome m . Given the values of m , one can define $\mathcal{S}(m)$ so that $|\Psi(m)\rangle$ is supported on the $+1$ eigenstate space of $\mathcal{S}(m)$ via appropriate relabelling $S_j \rightarrow \pm S_j$.

6.3 Logical operators

Next, we present the construction of a group of null operators

$$\mathcal{L} \equiv \left\langle P \in \text{Pauli} : \mathcal{C}(P) \in \mathcal{E} \right\rangle \quad (97)$$

and show that it is the logical operator group.

Again, the construction proceeds recursively. Here we denote the logical operator group constructed for P_t, \dots, P_1 by $\text{Logic}^{(t)}$. We start with

$$\text{Logic}^{(1)} = \text{Comm}(P_1) \equiv \left\langle P \in \text{Pauli} : [P, P_1] = 0 \right\rangle \quad (98)$$

where Comm represents the commutant. Here $\text{Comm}(P_1)$ contains 2^{2n-1} Pauli operators. We then recursively define

$$\text{Logic}^{(\tau)} \equiv \left\langle P_\tau, \{P \in \text{Logic}^{(\tau-1)} : [P, P_\tau] = 0\} \right\rangle. \quad (99)$$

In other words, we only keep Pauli operators which commute with P_τ and add P_τ instead. Observe that the stabilizer group $\mathcal{S}^{(\tau)}$ and $\mathcal{L}^{(\tau)}$ are constructed recursively in the same matter in Eq. (93) and Eq. (99) except that the initial sets are chosen differently, namely $\text{Logic}^{(1)} = \text{Comm}(\text{Stab}^{(1)})$.

The following lemma will be proven in appendix D.

Lemma 4. *We have*

$$\mathcal{L} = \text{Logic}^{(\tau)} \quad (100)$$

where $\text{Logic}^{(\tau)}$ is defined recursively via Eq. (99). Namely,

$$\mathcal{C}(P) \in \mathcal{E} \quad \text{iff} \quad P \in \text{Logic}^{(\tau)}. \quad (101)$$

Given the aforementioned construction of \mathcal{L} , it is immediate to prove that the logical operator group \mathcal{L} is nothing but the commutant of the stabilizer group \mathcal{S} .

Corollary 1. *The logical operator group \mathcal{L} is the commutant of the stabilizer group \mathcal{S} :*

$$\mathcal{L} = \text{Comm}(\mathcal{S}) = \{P \in \text{Pauli} : [P, Q] = 0 \ \forall Q \in \mathcal{S}\}. \quad (102)$$

Hence, null operators in \mathcal{L} play the role of logical operators when acting on the output wavefunction of a monitored Clifford circuit. In the next section, we will see this more clearly by constructing the Choi-Jamiołkowski state. Note that \mathcal{L} contains trivial logical operators (*i.e.* stabilizer operators) since $\mathcal{S} \subseteq \mathcal{L}$.

Here it is useful to recall that one can choose independent generators of \mathcal{L} as follows [34]:

$$\mathcal{L} = \left\langle \begin{bmatrix} \overline{Z_1} & \cdots & \overline{Z_k} & \overline{Z_{k+1}} & \cdots & \overline{Z_n} \\ \overline{X_1} & \cdots & \overline{X_k} & & & \end{bmatrix} \right\rangle \quad (103)$$

where operators commute with each other except for those in the same column. Namely, there always exist some Clifford unitary U which convert above Pauli operators into local ones via

$$\overline{X_j} = UX_jU^\dagger \quad \overline{Z_j} = UZ_jU^\dagger \quad (104)$$

up to possible ± 1 signs. Here, the stabilizer group \mathcal{S} is the center of \mathcal{L} :

$$\mathcal{S} = \langle \overline{Z_1}, \dots, \overline{Z_k} \rangle \quad (105)$$

since $\mathcal{S} = \text{Comm}(\mathcal{L})$. Here it is useful to note that the double commutant theorem holds for \mathcal{L}, \mathcal{S} , namely $\text{Comm}(\text{Comm}(\mathcal{S})) = \mathcal{S}$.

The number of elements in $\text{Logic}^{(\tau)}$ decreases only when P_τ satisfies $[P_\tau, \text{Stab}^{(\tau-1)}] = 0$ and $P_\tau \notin \text{Stab}^{(\tau-1)}$. Note that such decreases would correspond to loss of quantum information in the quantum error-correcting code interpretation. As we discussed in the previous subsection, this is not very likely to occur in the volume-law phase.

6.4 Examples

Below, we look at a few examples.

1) Assume that $P_j = Z_j$ for $j = 1, \dots, \tau$ ($\tau \leq n$). In this case, the stabilizer group is generated by

$$\text{Stab}^{(\tau)} = \langle Z_1, \dots, Z_\tau \rangle. \quad (106)$$

We also have

$$Z_j |\Psi(m)\rangle = m_j |\Psi(m)\rangle. \quad (107)$$

2) Assume that $n = 3$. Also assume that $P_1 = Z_1$, $P_2 = X_1$, $P_3 = Z_2$ and $P_4 = X_2$. We then have

$$\text{Stab}^{(1)} = \langle Z_1 \rangle, \quad \text{Stab}^{(2)} = \langle X_1 \rangle, \quad \text{Stab}^{(3)} = \langle X_1, Z_2 \rangle, \quad \text{Stab}^{(4)} = \langle X_1, X_2 \rangle \quad (108)$$

where anti-commuting generators are eliminated by adding P_2 and P_4 . Eigenvalues depend only on m_2 and m_4 :

$$X_1 |\Psi(m)\rangle = m_2 |\Psi(m)\rangle \quad X_2 |\Psi(m)\rangle = m_4 |\Psi(m)\rangle. \quad (109)$$

Logical operators can be found recursively

$$\begin{aligned}\text{Logic}^{(1)} &= \langle Z_1, X_2, Z_2, X_3, Z_3 \rangle, & \text{Logic}^{(2)} &= \langle X_1, X_2, Z_2, X_3, Z_3 \rangle \\ \text{Logic}^{(3)} &= \langle X_1, Z_2, X_3, Z_3 \rangle, & \text{Logic}^{(4)} &= \langle X_1, X_2, X_3, Z_3 \rangle\end{aligned}\tag{110}$$

which are commutants of stabilizer groups.

We can check that logical operators are null operators. For non-trivial logical operators X_3, Z_3 in $\text{Logic}^{(4)}$, we have

$$\mathcal{C}(X_3) = \mathcal{C}(Z_3) = (1, 1, 1, 1).\tag{111}$$

For stabilizer generators contained in $\text{Logic}^{(4)}$, we have

$$\mathcal{C}(X_1) = (-1, 1, 1, 1) = \mathcal{E}(P_2) \quad \mathcal{C}(X_2) = (1, 1, -1, 1) = \mathcal{E}(P_4).\tag{112}$$

3) Assume that $n = 2$. Also assume that $P_1 = Z_1$, $P_2 = Z_2$ and $P_3 = X_1X_2$. We then have

$$\text{Stab}^{(1)} = \langle Z_1 \rangle, \quad \text{Stab}^{(2)} = \langle Z_1, Z_2 \rangle, \quad \text{Stab}^{(3)} = \langle Z_1Z_2, X_1X_2 \rangle\tag{113}$$

where adding P_3 generated a larger stabilizer generator Z_1Z_2 . We also have

$$Z_1Z_2|\Psi(m)\rangle = m_1m_2|\Psi(m)\rangle \quad X_1X_2|\Psi(m)\rangle = m_3|\Psi(m)\rangle.\tag{114}$$

We have

$$\text{Logic}^{(1)} = \langle Z_1, X_2, Z_2 \rangle, \quad \text{Logic}^{(2)} = \langle Z_1, Z_2 \rangle, \quad \text{Logic}^{(3)} = \langle Z_1Z_2, X_1X_2 \rangle.\tag{115}$$

For operators in $\text{Logic}^{(3)}$, we see

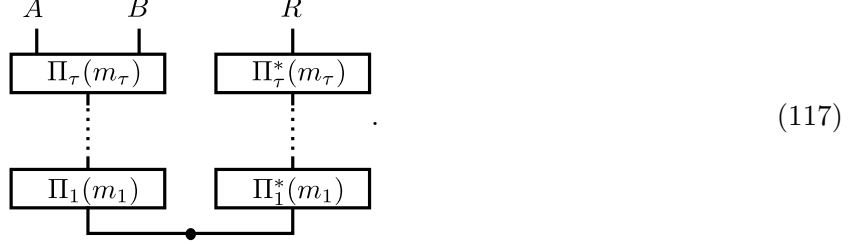
$$\mathcal{C}(Z_1Z_2) = (1, 1, 1) \quad \mathcal{C}(X_1X_2) = (-1, -1, 1).\tag{116}$$

7 Distilling the Choi-Jamiołkowski state

In this section, we will present an algorithm to distill an entangled state from the system and the reference R and show that it is identical to the Choi-Jamiołkowski state of the underlying stabilizer code.

7.1 Reverse error vector

The overall distillation procedure is graphically summarized as follows:



where we perform projective measurements of complex conjugates $\Pi^*(m)$. We then apply some appropriate feedback operation on R .

Recall that the original error vector $\mathcal{E}(P_j)$ was constructed by looking at commutation relations with P_i for $i < j$ in the past. Here, we instead need to introduce the reverse error vector $\mathcal{E}_{\text{rev}}(P_i)$ by looking at commutation relations with P_i for $i > j$. In other words, we only look at commutations with respect to Pauli operators in the future⁷. Namely, we define

$$\begin{aligned} \mathcal{E}_{\text{rev}}(P_i)_j &= 1 & (j < i) \\ \mathcal{E}_{\text{rev}}(P_i)_j &= \pm 1 & P_i P_j = \pm P_j P_i \quad (j \geq i). \end{aligned} \quad (118)$$

When $\mathcal{E}(P_i)_j$ and $\mathcal{E}_{\text{rev}}(P_i)_j$ are interpreted as matrices, they are related by transpose, namely

$$\mathcal{E}(P_i)_j = \mathcal{E}_{\text{rev}}(P_j)_i. \quad (119)$$

Let us denote the group generated by reverse error vectors as

$$\mathcal{E}_{\text{rev}} \equiv \langle \{ \mathcal{E}_{\text{rev}}(P_j) \} \rangle. \quad (120)$$

In appendix E, we will prove the following lemma.

Lemma 5. *In the distillation algorithm from Eq. (117), measurement of $s (= m \cdot \overline{m})$ occurs if and only if*

$$s \in \mathcal{E}_{\text{rev}}. \quad (121)$$

This lemma suggests that, given $s = m \cdot \overline{m}$, one can always find a set of indices $\Lambda \subseteq \{1, \dots, \tau\}$ such that

$$s = \prod_{j \in \Lambda} \mathcal{E}_{\text{rev}}(P_j) \quad (122)$$

where \prod represents component-wise multiplications of vectors. The necessary feedback operation is

⁷While we do not have an intuitive explanation for the need of reverse error vectors, one possible hint may be obtained by observing $\mathcal{C}(P_j) = \mathcal{E}_{\text{rev}} \cdot \mathcal{E}(P_j)$. A mathematical reason for considering the reverse error vector is presented in appendix E.

given by

$$P_\Lambda \equiv \prod_{j \in \Lambda} P_j. \quad (123)$$

We then have the following result.

Lemma 6. *The output of the aforementioned distillation algorithm for the system-reference entanglement is*

$$\mathbb{E}(\sigma_{AB\overline{AB}}) = \frac{1}{N_S} \sum_{P \in \mathcal{S}} |P\rangle\langle P| \quad (124)$$

where N_S is the number of elements in \mathcal{S} .

The proof of this lemma is presented in appendix E.

7.2 Choi-Jamiołkowski state

Let $P \in \mathcal{L}$ be a Pauli operator in the logical operator group. Then the output state from the distillation algorithm satisfies

$$\text{Tr} \left[(P \otimes P^*) \mathbb{E}(\sigma_{AB\overline{AB}}) \right] = 1 \quad (125)$$

since stabilizer generators commute with P . This implies that the output state $\mathbb{E}(\sigma_{AB\overline{AB}})$ satisfies

$$\langle \overline{Z}_j \otimes \overline{Z}_j^* \rangle = 1 \quad \langle \overline{X}_j \otimes \overline{X}_j^* \rangle = 1 \quad j = 1, \dots, k. \quad (126)$$

Hence, k EPR pairs can be distilled from AB and \overline{AB} , and $\overline{X}_j, \overline{Z}_j$ for $j = 1, \dots, k$ transform encoded quantum information by acting as Pauli X and Z operators on logical qubits. On the other hand, we have

$$\langle \overline{Z}_j \otimes \overline{Z}_j^* \rangle = 1 \quad \langle \overline{X}_j \otimes \overline{X}_j^* \rangle = 0 \quad j = k+1, \dots, n. \quad (127)$$

Here \overline{X}_j for $j = k+1, \dots, n$ are defined as anti-commuting partners of \overline{Z}_j . This suggests that AB and \overline{AB} retains classical correlation with respect to eigenvalues of \overline{Z}_j and \overline{Z}_j^* .

The classical correlation in $\mathbb{E}(\sigma_{AB\overline{AB}})$ results from averaging over m . If one looks at the distilled state for each m , we find that

$$\langle \overline{Z}_j \otimes I \rangle = \langle I \otimes \overline{Z}_j^* \rangle = 1 \quad \text{for } \sigma_{AB\overline{AB}}(m). \quad (128)$$

Here we assumed that \overline{Z}_j is properly relabelled so that the output state is stabilized by $\mathcal{S}(m)$ where the expectation values are taken with respect to $\sigma_{AB\overline{AB}}(m)$. Note that Eq. (126) holds for each $\sigma_{AB\overline{AB}}(m)$ as well. Hence, we can conclude that $\sigma_{AB\overline{AB}}(m)$ is nothing but the Choi-Jamiołkowski state of a stabilizer code with the stabilizer group $\mathcal{S}(m)$.

Applying this version of the distillation algorithm to the Gullans-Huse proposal will distill an EPR pair in the encoded basis states instead of a pair of qubits.

8 State-independent entanglement structure

We have developed a theoretical framework to study the entanglement structure of monitored quantum circuits and derived several rigorous results. In the remainder of the paper, we discuss its implications on the physics of monitored quantum circuits in the volume-law phase.

In this section, we argue that the entanglement structure of a monitored quantum circuit changes drastically when the subsystem size A exceeds a certain critical size, which can be identified as the code distance d_{code} . While we do not focus on specific models of monitored circuits, it will be useful to imagine random monitored Clifford circuits in the volume-law phase which has been running for longer than the entanglement equilibrium time to develop the volume-law entanglement, but shorter than the exponentially long quantum memory time.

8.1 Decoupling and state-independence

So far we have used a maximally mixed state as an initial state of monitored quantum circuits (or equivalently, we have appended the entangled reference system R). A naturally arising question concerns the entanglement structure when a pure state, instead of a maximally mixed state, is prepared as an initial state. Here we argue that entanglement between two subsystems A and B is largely independent of the choice of initial states as long as the size of the smaller subsystem A is below a certain critical size which plays the role of the code distance d_{code} of a monitored quantum circuit.

Let us begin by recalling the notion of decoupling (see [35] for rigorous arguments). Assume that a smaller subsystem A is strongly entangled with B , namely

$$I_{(A,B)} \approx 2S_A. \quad (129)$$

Here note that $I_{(A,B)} \leq 2S_A$. Recalling $I_{(A,B)} + I_{(A,R)} = 2S_A$ for a pure state on ABR , we then notice that the subsystem A is almost completely decoupled from the reference R with $I_{(A,R)} \approx 0$ ⁸. This suggests that entanglement between A and B are largely independent of the initial state of the circuit. To be concrete, let us pick some pure state, such as product states or Haar random states, as an initial state of a monitored quantum circuit. This situation can be realized by performing a projective measurement on the reference system R . Namely, if we project R onto $|\psi^*\rangle$, then the initial state on the system AB will be set to $|\psi\rangle$. Since the reference R is decoupled from A , quantum operations on R cannot make a significant influence on the entanglement between A and B . As such, the entanglement between A and B is largely independent of initial states⁹.

Now, recall that a monitored quantum circuit in the volume-law phase can be interpreted as a quantum error-correcting code that is robust against local projective measurements. This suggests that logical operators of the code cannot be supported on a small subsystem. Namely, if the subsystem A is smaller than the code distance d_{code} , we expect to have

$$I_{(A,R)} \approx 0 \quad \text{when} \quad |A| < d_{\text{code}} \quad (130)$$

since, otherwise, an approximate logical operator can be constructed on A . The above equation can be

⁸A conventional definition of decoupling is $\rho_{AR} \approx \rho_A \otimes \rho_R$. Here we use the word “decoupling” in a loose sense by referring to the situation with small $I_{(A,R)}$. To obtain a useful quantitative decoupling inequality, it is often more convenient to use Rényi generalizations of mutual information which can be accessed from OTOCs [36].

⁹Since $I_{(A,R)}$ is not exactly zero, there may exist fine-tuned initial states which generate atypical entanglement.

interpreted as a definition of the approximate code distance. Indeed, it is useful to recall that conditions for approximate error-correction can be expressed in terms of the coherent information, which can be also interpreted as the conditional entropy $S_{A|R}$ [37]. This observation suggests that the entanglement structure of a monitored quantum circuit is largely independent of initial states up to the size scale of the code distance d_{code} due to decoupling.

8.2 Estimate of the code distance

The code distance d_{code} depends on the specifics of the model of interest. Here we argue that, for a monitored quantum circuit in the volume-law phase with an exponentially long memory time, the code distance d_{code} scales polynomially with respect to the system size n ¹⁰.

We begin with the cases of Clifford circuits. In a stabilizer quantum error-correcting code, there always exists a subsystem A consisting of d_{code} qubits which support a non-trivial Pauli logical operator $\ell = P_{A_1} \otimes P_{A_2} \otimes \cdots \otimes P_{A_{d_{\text{code}}}}$. Suppose that one performs projective measurements with some finite probability $p > 0$. The quantum information associated with the logical operator ℓ will be lost when one accidentally measures $P_{A_1} \otimes P_{A_2} \otimes \cdots \otimes P_{A_{d_{\text{code}}}}$. This event occurs with probability

$$\left(\frac{p}{3}\right)^{d_{\text{code}}}. \quad (131)$$

Hence a monitored circuit will lose a piece of quantum information in one unit of time at least with the probability in Eq. (131). This suggests that the quantum memory time is upper bounded by

$$t_{\text{memory}} \lesssim \left(\frac{3}{p}\right)^{d_{\text{code}}} \quad (132)$$

which sets a lower bound on d_{code} :

$$\log(t_{\text{memory}}) \lesssim d_{\text{code}} \log\left(\frac{3}{p}\right). \quad (133)$$

Therefore, in order to have an exponential quantum memory time, the code distance d_{code} needs to scale polynomially with respect to the total system size n ¹¹:

$$d_{\text{code}} = \text{Poly}(n). \quad (134)$$

It is worth noting that the above analysis only gives a lower bound on d_{code} , and hence does not give a sufficient condition for an exponential memory time.

For non-Clifford circuits, logical operators cannot be written as a tensor product of Pauli operators, so the above argument is not readily applicable. Here, we argue that a similar lower bound still applies based on the relation between random Clifford and Haar random unitary operators. Recall that, in monitored Clifford circuits, the loss of quantum information occurs in a discrete manner in time steps. Namely, when the mutual information $I(AB, R)$ decreases, its value drops by an integer, while for other times, $I(AB, R)$ may stay constant. Only when one considers the behavior of $I(AB, R)$ averaged over all the statistical realizations of random Clifford circuits, continuous decays by non-integer

¹⁰From the conventional wisdom on phase transitions, it will be natural to expect an exponential memory time when the system is away from the criticality of the entanglement phase transition.

¹¹Here, by an exponential memory time, we mean that t_{memory} grows as $\simeq \exp(n^\gamma)$ with $\gamma > 0$.

values can be found. This is because, for Clifford circuits, the sample-to-sample variance is large. For monitored quantum circuits driven by non-Clifford dynamics, we expect that the decrease of $I(AB, R)$ will be continuous. This intuition is based on an observation that the statistical average for random Clifford dynamics converges to the result from a single realization of Haar random circuits due to the concentration of measure (which can be verified by computing the variance). Hence, we conclude that, for non-Clifford circuits, the mutual information $I(AB, R)$ will decrease continuously over the period of t_{memory} , and as such, the code distance d_{code} should be polynomial in n .

Finally, let us note that Li and Fisher investigated the code distance¹² of one-dimensional random monitored Clifford circuits and numerically obtained an estimate of $d_{\text{code}} \sim n^{0.36}$ [22] (see [19] for an estimate from an earlier work which qualitatively match with this estimate).

With these observations and previous results, we conclude that the entanglement structure of a monitored quantum circuit in the volume-law phase is independent of initial states up to a $\text{Poly}(n)$ size scale which is of the order of the code distance.

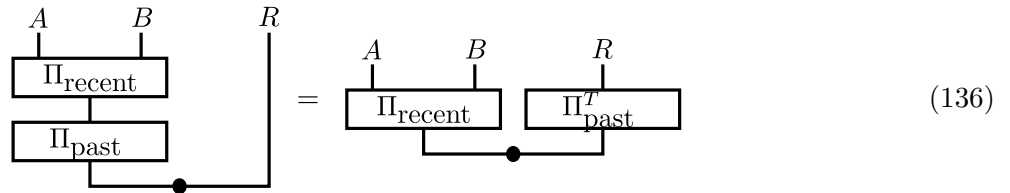
8.3 Measurement history dependence

Finally, we discuss how the entanglement depends on measurement outcomes in the past. Namely, we will argue that measurements in the distant past are largely irrelevant to the entanglement between two subsystems A and B when A is smaller than d_{code} .

Let us split the measurement operator $\Pi(m)$ into two parts $\Pi(m) = \Pi_{\text{recent}}(m_{\text{recent}})\Pi_{\text{past}}(m_{\text{past}})$ where

$$\begin{aligned}\Pi_{\text{recent}}(m_{\text{recent}}) &\equiv \Pi_{\tau}(m_{\tau}) \cdots \Pi_{\tau-\Delta\tau}(m_{\tau-\Delta\tau}) \\ \Pi_{\text{past}}(m_{\text{past}}) &\equiv \Pi_{\tau-\Delta\tau-1}(m_{\tau-\Delta\tau-1}) \cdots \Pi_1(m_1).\end{aligned}\tag{135}$$

The output wavefunction can be expressed in the following manner



$$\tag{136}$$

where we moved $\Pi_{\text{past}}(m_{\text{past}})$ to the right hand side by taking transpose. Written in this form, we can interpret the above wavefunction as an output wavefunction from $\Pi_{\text{recent}}(m_{\text{recent}})$ whereas $\Pi_{\text{past}}(m_{\text{past}})$ acts as a projection on the reference R . (In other words, the portion of $\Pi_{\text{past}}(m_{\text{past}})$ can be interpreted as the initial state of $\Pi_{\text{recent}}(m_{\text{recent}})$).

Here we assume that $\Delta\tau$ is longer than the entanglement equilibrium time so that the subsystem A , which is smaller than the code distance d_{code} , is decoupled from the reference R . From arguments in previous subsections, we find that the entanglement between A and B is immune to projective measurements on the reference R . Hence, we can conclude that the measurements in the distant past $\Pi_{\text{past}}(m_{\text{past}})$ does not affect the entanglement between A and B . This suggests that the entanglement between A and B can be distilled without knowing m_{past} . As such, the entanglement structure below the

¹²Strictly speaking, Li and Fisher studied the contiguous code distance, instead of the conventional code distance, by looking at single intervals only.

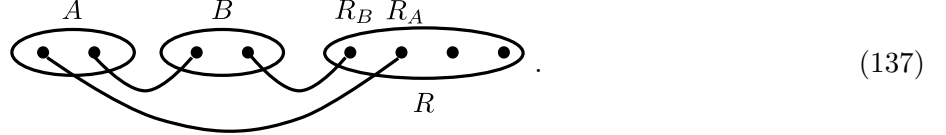
d_{code} scale depends only on measurements that occurred within the entanglement equilibrium time ¹³.

9 State-dependent entanglement structure

Once the subsystem A becomes larger than the code distance d_{code} , the mutual information $I_{(A,R)}$ may take a non-zero value. In this case, the entanglement structure between A and B will be dependent on the initial states of the monitored quantum circuit as well as measurement outcomes in the distant past. Here, we present a heuristic argument concerning how the mutual information $I_{(A,B)}$ changes by preparing a generic pure state as an initial state instead of the maximally mixed state.

9.1 Entanglement swapping by random projection

In order to gain some insight, it is useful to consider a simplified toy model of the entanglement structure involving A, B, R as shown below:



where bipartite entanglement (*e.g.* EPR pairs) are distributed among A, B, R . The bipartite entanglement between A and B represents the state-independent entanglement which exists below the d_{code} scale whereas the $A - R$ and $B - R$ entanglement are associated with the encoding of logical qubits, and can be accessed only above the d_{code} scale. Here R_A and R_B represent degrees of freedom which are entangled with A and B respectively.

Let us think of projecting R onto some pure state $|\psi\rangle_R$. If $|\psi\rangle$ is a product state on $R_A \otimes R_B$, the projection will not generate any additional entanglement, and the value of $I_{(A,B)}$ remains unchanged. On the other hand, if $|\psi\rangle$ is entangled across R_A and R_B (*e.g.* an EPR pair on $R_A \otimes R_B$), the projection will lead to additional entanglement:



Namely, the original entanglement between A and R is merged with the entanglement between B and R , and then contributes as additional entanglement between A and B . Note that this additional entanglement depends on how A, B were entangled with R , as well as the choice of the entangled state $|\psi\rangle_R$ on R .

¹³For one-dimensional random monitored circuits with product initial states (*e.g.* $|0\rangle^{\otimes n}$), it will take $O(n)$ time in order to reach the entanglement equilibrium with the volume-law entanglement [2]. A recent study in [38], however, seems to suggest that it will take only $O(n^{\frac{2}{3}})$ time in order to reach the steady value of the entanglement entropy if one starts with a maximally mixed state instead of product states. This is due to the observation that the entangling minimal surface of a subsystem A extends into the bulk with the depth $\sim |A|^{\frac{2}{3}}$ only, instead of $\sim |A|$. As such, the decoupling with $I(A, R) \approx 0$ will occur in $O(n^{\frac{2}{3}})$ time instead of $O(n)$. We speculate that this is due to a possibility that the size of stabilizer generators may grow faster than linear in the presence of projective measurements where multiple stabilizer generators may need to be combined to form new stabilizer generators. This will not lead to any causality violation since the verification of entanglement needs to know the measurement outcomes which can travel only at the speed of light.

This mechanism can be interpreted as the quantum teleportation (or the entanglement swapping). Namely, Bell measurements on R_A and R_B can send R_A to a subsystem B by using the $B - R_B$ entanglement as a resource. This forces the qubits on A , which were initially entangled with R_A , to be entangled with B . In other words, the $A - R$ entanglement was swapped to become the $A - B$ entanglement.

As this observation suggests, collapsing R into an entangled state tends to increase the mutual information $I_{(A,B)}$. One can make this observation more rigorous by considering a projection onto a Haar random state on R . Namely, one can show that the Rényi-2 entanglement entropy $S_A^{(2)}$ does not change much after projecting R onto a random state (assuming A is the smaller subsystem). Consider the following output state with Haar random initial state $|\psi\rangle$:

$$\frac{1}{\sqrt{\text{Prob}(m)}} \begin{array}{c} A \quad B \\ \boxed{\Pi(m)} \\ \downarrow \\ |\psi\rangle \end{array} \quad (139)$$

where the numerical factor $\frac{1}{\sqrt{\text{Prob}(m)}}$ achieves approximately proper normalization. Let us denote the density matrix of the above wavefunction by $\rho_{|\psi\rangle\langle\psi|}$. Then we have

$$\text{Tr}(\rho_A^2_{|\psi\rangle\langle\psi|}) = \frac{1}{\text{Prob}(m)^2} \begin{array}{c} A \quad B \\ \boxed{\Pi(m)} \\ \downarrow \\ |\psi\rangle\langle\psi| \\ \downarrow \\ \boxed{\Pi^\dagger(m)} \\ \downarrow \\ A \quad B \\ \boxed{\Pi(m)} \\ \downarrow \\ |\psi\rangle\langle\psi| \\ \downarrow \\ \boxed{\Pi^\dagger(m)} \end{array} \quad (140)$$

Taking the Haar average leads to

$$\int d|\psi\rangle \text{Tr}(\rho_A^2_{|\psi\rangle\langle\psi|}) = \frac{d}{d+1} \left(\text{Tr}(\rho_A^2) + \text{Tr}(\rho_B^2) \right) \quad (141)$$

where ρ_A and ρ_B are defined for the original output wavefunction that includes the entangled reference R .

Here we assumed that A is the smaller subsystem. Hence, it is natural to assume

$$\text{Tr}(\rho_B^2) \ll \text{Tr}(\rho_A^2). \quad (142)$$

Recalling that $d = 2^n$, we find that $S_A^{(2)}$ stays approximately the same after projecting R onto Haar

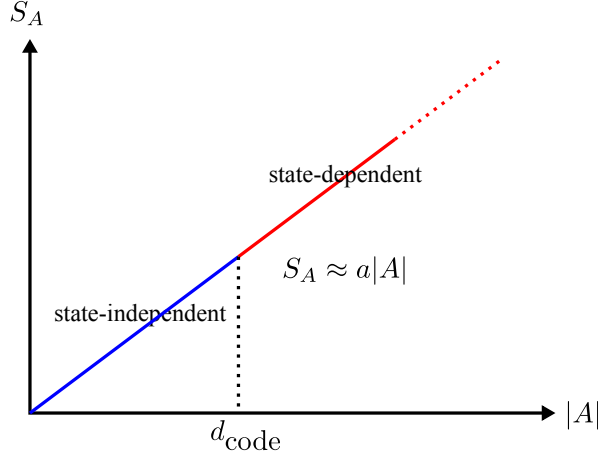


Figure 4: The volume-law scaling in the volume-law phase. The overall behavior of S_A does not depend on the initial states (except atypical ones) due to the entanglement swapping. Across the d_{code} scale, however, the entanglement changes from being state-independent to state-dependent. We expect that the complexity of the entanglement verification changes drastically.

random states:

$$S_{A|\psi\rangle\langle\psi|}^{(2)} \approx S_A^{(2)}. \quad (143)$$

While this analysis computed Rényi-2 entropy, we expect that the entanglement entropy behaves similarly. This suggests that the value of $I_{(A,B)}$ will increase roughly by $I_{(A,R)}$, namely

$$I_{(A,B)} \text{ with random } R \text{ projection} \approx I_{(A,BR)} \text{ with no } R \text{ projection}. \quad (144)$$

Hence, after the random projection on R , the subsystem A will be entangled with B without losing its initial entanglement with BR . This increase of $I_{(A,B)}$ can be viewed as the entanglement swapping by a random projection.

We speculate that the above conclusion for Haar random initial states also applies to the cases when product states are chosen as initial states, since the degrees of freedom R_A and R_B will be non-local on the reference system R , and thus projecting R onto a product state has an effect of projecting R_A and R_B (as well as their complementary systems) onto entangled states. Hence we expect that the value of the entanglement entropy S_A is largely independent of the initial states (except fine-tuned ones), as in Fig. 4. This observation is consistent with previous numerical and analytical results, see [22] for instance. This provides an important caution that the volume-law scaling of the entanglement entropy $S_A \approx a|A|$ is too crude to this subtle, yet important difference of the entanglement structure below and above the code distance scale. In the next section, we will argue that the subleading contribution to the entanglement entropy probes coding properties of a monitored quantum circuit.

9.2 On complexity of entanglement verification

One salient feature of the state-independent entanglement below the d_{code} scale is that its verification does not require knowledge of measurement outcomes in the distant past. This suggests that the quantum complexity of the entanglement verification may change drastically across the d_{code} scale. Indeed,

for Clifford monitored circuits, when a subsystem A is smaller than d_{code} , the distillation algorithm can run in a time scale comparable to the entanglement equilibrium time which is polynomial in the system size. For subsystems larger than d_{code} , however, the algorithm needs to know measurement outcomes in the distance past as well as the initial state. This suggests that the distillation complexity can be large if the circuit has been running for much longer than the entanglement equilibrium time¹⁴. As such, for monitored Clifford circuits, there will be a “phase transition” of the entanglement verification complexity across the d_{code} scale [39]¹⁵.

9.3 Does measurement destroy entanglement?

Discussions so far reveal a certain tension between the conventional understanding of the physics of monitored quantum circuits and the role of projective measurements concerning the emergence of the volume-law entanglement. It is commonly believed that projective measurements in monitored quantum circuits lead to decoherence which *destroys* entanglement. Namely, the conventional understanding of the emergence of the volume-law entanglement is that the effect of scrambling dynamics, which create entanglement, can outperform the decoherence from local projective measurements. This intuition can be made concrete by recalling the simplified toy model of monitored quantum circuits with intermittent projective measurements due to Choi *et al.* [18]. In this toy model, the system is separated into groups of multiple qubits where neighboring groups of qubits interact with each other via random unitaries. Once neighboring groups of qubits are thoroughly mixed, local projective measurements are performed. In this toy model, random unitary dynamics can encode preexisting entanglement into subspaces of quantum error-correcting codes which protect the volume-law entanglement from local projective measurements.

As the above observation from the toy model suggests, projective measurements appear to destroy entanglement. However, this lesson should be understood with caution. As we have discussed throughout this paper, two subsystems A and B can be entangled in a state-independent manner due to the decoupling phenomena induced by projective measurements. Specifically, let us consider the case where the initial state is a maximally mixed state $\mu_A \otimes \mu_B = \frac{1}{d} I_A \otimes I_B$. Observe that, if no measurements were performed, then the system would remain unentangled because $\mu_A \otimes \mu_B$ is invariant under the action of any unitary operator. Once projective measurements are performed, however, the output quantum state can start to develop entanglement between A and B . Hence, in this case with a maximally mixed initial state, local projective measurements *create* entanglement, instead of destroying it. One might think that this has to do with the special case of a maximally mixed initial state, but the entanglement structure between A and B is independent of the initial states.

A naturally arising question then is whether projective measurements destroy or create entanglement. The resolution of this apparent tension is immediate from discussions in previous subsections. Below the code distance scale, the entanglement structure is independent of the initial states, and thus projective measurements are indeed creating entanglement via the decoupling phenomena. Above the code distance scale, on the other hand, the subsystem in the output wavefunction starts to be correlated with the initial states. In this regime, it is reasonable to view the monitored circuit as an encoding into a quantum error-correcting code which protects entanglement from projective measurements which would destroy entanglement. Hence, projective measurements can create or destroy entanglement, depending on the

¹⁴While an arbitrary Clifford operator can be implemented efficiently on a quantum computer, we expect that processing exponentially many measurement outcomes cannot be done efficiently.

¹⁵If one hopes that the entanglement in monitored quantum systems would ever be relevant to physically observable phenomena, it must be verifiable. In this regard, one may speculate that the state-independent entanglement below the d_{code} scale will be responsible for such a phenomena (if exists).

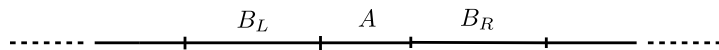


Figure 5: An heuristic argument showing $\gamma = \gamma_{\text{code}}$.

size scale of interest. Furthermore, from this perspective, we argue that the toy model from [18] captures the coarse-grained physics of monitored quantum circuits above the code distance scale.

10 Code distance from sub-leading entropy

Observations from the previous sections resolve a certain puzzle concerning the sub-leading contribution to the volume-law entanglement entropy in a monitored quantum circuit.

Several previous works have conjectured that, in the volume-law phase of a monitored quantum circuit, there will be a logarithmic sub-leading contribution to the volume-law entanglement [21, 40]. Namely, for one-dimensional circuits, the following form of asymptotic entanglement scaling has been conjectured:

$$S_A = aL_A + c \log L_A. \quad (145)$$

Certain physical arguments to explain the origin of the logarithmic term have been presented in [21, 40] based on size distributions of stabilizer generators and an entropy drop via projective measurements. However, Li and Fisher, who numerically studied a one-dimensional Clifford circuit in a later work [22], have found that there is another sub-leading contribution, namely

$$S_A = aL_A + bL_A^\gamma + c \log L_A \quad (146)$$

with some exponent $\gamma \approx 0.38$. Here L_A is the length of A .

Here we present a heuristic argument showing that the sub-leading term $\sim L_A^\gamma$ results from coding properties of the underlying monitored quantum circuit¹⁶. Namely, we claim that the exponent γ is equal to the exponent for the code distance $d_{\text{code}} \sim L^{\gamma_{\text{code}}}$:

$$\gamma = \gamma_{\text{code}}. \quad (147)$$

Let us pick three neighboring subsystems B_L , A and B_R such that $B = B_L \cup B_R$ surrounds A (Fig. 5). Let L_A and L_B be the lengths of A and B_L, B_R respectively. Let us compute the mutual information $I_{(A,B)}$ by using the asymptotic entanglement scaling formula in Eq. (146). We have

$$S_A \approx aL_A + bL_A^\gamma \quad S_{B_L} \approx S_{B_R} \approx aL_B + bL_B^\gamma. \quad (148)$$

¹⁶In a recent work [38], Li, Vijay and Fisher utilized an effective theory description of one-dimensional monitored quantum circuits and attributed the origin of the $\sim L_A^\gamma$ term as a fluctuation of the entangling surface.

We also have

$$S_{AB} \approx a(L_A + 2L_B) + b(L_A + 2L_B)^\gamma. \quad (149)$$

Finally, we need to compute S_B . At this moment, let us assume that B_L and B_R are not entangled with each other since B_L and B_R are separated by A . (We will return to this assumption in a few paragraphs). Then, we have

$$S_B \approx S_{B_L} + S_{B_R} \approx 2aL_B + 2bL_B^\gamma. \quad (150)$$

Using these asymptotic estimates, we obtain

$$I_{(A,B)} \approx bL_A^\gamma + 2bL_B^\gamma - b(L_A + 2L_B)^\gamma \quad (151)$$

where the volume terms cancel with each other.

Let us fix L_A and increase L_B . As L_B becomes larger than L_A , the above estimate can be further approximated by

$$I_{(A,B)} \approx bL_A^\gamma + 2bL_B^\gamma - b(2L_B)^\gamma \left(1 + \gamma \frac{L_A}{2L_B}\right) \approx b(2 - 2^\gamma)L_B^\gamma. \quad (152)$$

So, $I_{(A,B)}$ grows with the exponent γ as we increase L_B . However, $I_{(A,B)}$ is upper bounded by $2S_A \approx 2aL_A$, so we expect that $I_{(A,B)}$ will get saturated when

$$L_A \approx L_B^\gamma \quad (153)$$

where we ignored the constants a, b . Hence, as long as $L_B \gg L_A^{\frac{1}{\gamma}}$, two subsystems A and B are nearly maximally entangled, and A is decoupled from the reference R . In summary, we have obtained the following estimate:

$$\begin{aligned} I_{(A,B)} &\approx L_B^\gamma & (L_B \lesssim L_A^{\frac{1}{\gamma}}) \\ &\approx L_A & (L_B \gtrsim L_A^{\frac{1}{\gamma}}). \end{aligned} \quad (154)$$

Now we think of increasing both L_A and L_B . Recall that the value of L_B is upper bounded by the system size L . Then, if $L_A \gtrsim L^\gamma$, one cannot take a large enough subsystem B such that $I_{(A,R)} = 0$. Namely, we expect that A will be entangled with the reference R once L_A becomes larger than L^γ . Hence, we can conclude that the code distance scales as

$$d_{\text{code}} \approx L^\gamma \quad \text{and} \quad \gamma = \gamma_{\text{code}}. \quad (155)$$

For one-dimensional random monitored Clifford circuits, Li and Fisher numerically estimated $\gamma \approx 0.36$ and $\gamma_{\text{code}} \approx 0.38$ which is consistent with this argument.

Since $I_{(A,B)}$ is upper bounded by $2S_A$, our estimate of the mutual information in Eq. (152) is valid only for $L_B \lesssim L_A^{\frac{1}{\gamma}}$. When $L_B \gtrsim L_A^{\frac{1}{\gamma}}$, we expect that our assumption of $S_B \approx S_{B_L} + S_{B_R}$ in Eq. (150) becomes invalid. In order to verify this expectation, we will evaluate the mutual information between

B_L and B_R . Let us begin by computing the mutual information between B_L and AB_R . We have

$$I_{(B_L, AB_R)} = S_{B_L} + S_{AB_R} - S_{B_L AB_R} \approx bL_B^\gamma + b(L_A + L_B)^\gamma - b(L_A + 2L_B)^\gamma \approx b(2 - 2^\gamma)L_B^\gamma. \quad (156)$$

The mutual information $I_{(B_L, B_R)}$ can be lower bounded by using the generic upper bound on the conditional mutual information:

$$2S_A \geq I_{(B_L, AB_R)} - I_{(B_L, B_R)}. \quad (157)$$

This leads to

$$I_{(B_L, B_R)} \gtrsim b(2 - 2^\gamma)L_B^\gamma - 2aL_A. \quad (158)$$

The lower bound Eq. (158) becomes non-trivial for $L_B \gtrsim L_A^{\frac{1}{\gamma}}$, which is exactly when we expect that the assumption of $S_B \approx S_{B_L} + S_{B_R}$ starts to become invalid due to the saturation of $I_{(A, B)}$. Here we expect that this lower bound is saturated¹⁷. Hence we obtain

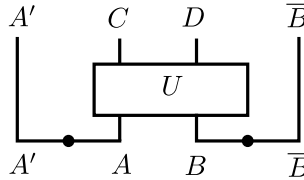
$$\begin{aligned} I_{(B_L, B_R)} &\approx 0 & (L_B \lesssim L_A^{\frac{1}{\gamma}}) \\ &\approx L_B^\gamma & (L_B \gtrsim L_A^{\frac{1}{\gamma}}). \end{aligned} \quad (159)$$

Here, strictly speaking, $I_{(B_L, B_R)} \approx 0$ means that $I_{(B_L, B_R)}$ is smaller than L_B^γ in an asymptotic sense.

11 Relation to black hole physics

In this section, we establish a connection between monitored quantum circuits and black hole physics. Let us begin by arguing that monitored quantum circuits can be viewed as the Hayden-Preskill recovery problem running backward in time [32].

The Hayden-Preskill recovery problem asks whether a piece of quantum information thrown into an old black hole, which is maximally entangled with the early radiation, can be retrieved by having access to both the early and late radiations. Information theoretically, this problem can be formulated as the following wavefunction



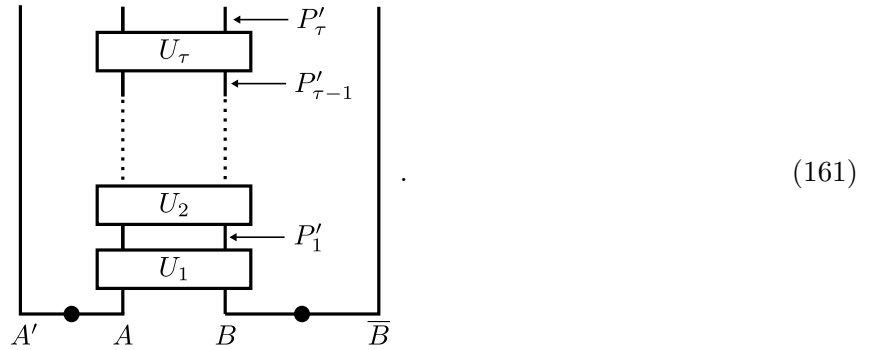
$$\quad (160)$$

¹⁷For Clifford circuits, the saturation of Eq. (158) can be argued by studying the sizes of stabilizer generators. In order to compute $I(B_L, B_R)$, we need to find the number of stabilizer generators which are supported non-locally over B_L and B_R . Eq. (156) suggests that there are $b(2 - 2^\gamma)L_B^\gamma$ independent stabilizer generators which are supported non-locally over B_L and AB_R . Given such a non-local stabilizer over B_L and AB_R , we look at the profile of Pauli operators on A . If its support on A belongs to the local stabilizer group \mathcal{S}_A on A , the stabilizer generator can be brought into a form non-locally supported over B_L and B_R , and hence it will make a contribution to $I(B_L, B_R)$. By noting that the profile of operators on A must commute with \mathcal{S}_A , one notices that the number of such stabilizer generators can be lower bounded by $b(2 - 2^\gamma)L_B^\gamma - 2S_A$, which is identical to Eq. (158). The asymptotic saturation of this inequality can be argued by assuming that the Pauli operator profile of these stabilizer generators are random (with the constraint that they commute with \mathcal{S}_A).

where the old black hole is modelled as n_B copies of EPR pairs on B and \bar{B} with \bar{B} being the early radiation. The infalling quantum state is represented by EPR pairs on A and A' where A' plays the role of the reference system. The system evolves by some unitary operator U , and C and D represent the remaining black hole and the late radiation respectively. In an information theoretic language, the Hayden-Preskill recovery problem asks whether quantum entanglement can be distilled from A' and $\bar{B}D$.

Hayden and Preskill pointed out that the information is recoverable as long as $n_D \gtrsim n_A$ when the dynamics U is a Haar random unitary operator [41]. Later, it has been found that the information is recoverable when the black hole's dynamics is scrambling as quantified by OTOC functions [17, 29, 42]. Since the black hole scrambles quantum information, this result provides a formal proof that information can indeed leak out from an old black hole due to scrambling dynamics. Several concrete methods of retrieving quantum information from an old black hole have been proposed [17, 43–48].

Here, instead of collecting the late Hawking radiations, let us think of performing projective measurements on late radiations in a continuous manner. This can be schematically represented as follows:



The central question is whether the quantum information is recoverable from the early radiation \bar{B} as a result of projective measurements or not. In other words, we are interested in whether A and B are entangled or not.

One may be able to see the similarity between this quantum circuit and the monitored circuit. Let us think of “turning” the diagram upside down so that the time flows backward (from the up to the bottom) and two subsystems AB become the output of the quantum circuit. Then, one can see that the Hayden-Preskill recovery problem with continuous measurement is identical to the entanglement distillation problem in the monitored quantum circuit. Here the subsystem A and B in monitored quantum circuits correspond to the infalling quantum state and the early radiation in the Hayden-Preskill recovery problem respectively. As such, emergence of the volume-law entanglement in monitored quantum circuits can be interpreted as information recovery from an old black hole via projective measurements of outgoing radiations.

Furthermore, the entanglement distillation algorithm can be converted into an algorithm to reconstruct the initial quantum information that was thrown into an old black hole. For the case of Clifford

dynamics, the recovery algorithm is given by

(162)

where the dual code will be constructed by reversing the flow of the time. After applying an appropriate feedback Pauli operator, EPR pairs will be distilled on A' and $\overline{A'}$.

The physics of monitored quantum circuits also provides us with useful insights into the problem of the black hole interior reconstruction. Understanding the black hole interior will be essential in resolving various puzzles concerning the quantum nature of black holes. According to Hawking's semiclassical calculation, there must exist pairs of entangled Rindler modes across the black hole horizon. Then, the modes inside the black hole can then be defined unambiguously in the outside quantum mechanics language as an entangled partner of the outgoing mode. As such, explicitly writing down degrees of freedom that are entangled with the outgoing mode is an important issue.

A monitored quantum circuit can be interpreted as a toy model of the interior reconstruction problem where the black hole is continuously measured by outside observers [49]. Namely, the subsystem A can be viewed as the outgoing mode, and finding degrees of freedom, which are entangled with A , is equivalent to identifying the interior partner mode. Here R can be viewed as the early Hawking radiation that was entangled with the black hole initially. When a black hole remains unperturbed with no projective measurement, the outgoing mode A is entangled with the reference system R , which suggests that the interior partner mode can be found on R . When a black hole is continuously monitored, the outgoing mode A will be decoupled from the reference system R , and will be entangled with the complementary subsystem B . This suggests that the interior partner mode can be written in a state-independent manner by using degrees of freedom on B only. Namely, the same construction of the interior partner mode works for the cases where the black hole's initial state was a pure state.

12 Outlook

In this paper, we have investigated the entanglement structure in monitored Clifford circuits and presented a method of verifying the entanglement. The main technical tool was the use of a dual classical error-correcting code whose codewords correspond to the spacetime patterns of the operator growth measured by OTOCs. We have also applied the developed framework to study the coding properties of monitored Clifford circuits. Finally, we have applied our technical results to various physical questions and puzzles. We hope that theoretical techniques developed in this paper will be useful in further addressing various important open problems concerning monitored Clifford circuits and beyond. Below we discuss some possible future problems.

We have presented a simple deterministic entanglement distillation algorithm that enables us to verify quantum entanglement between two subsystems in a monitored Clifford circuit. We expect that this algorithm can be readily employed for experimental demonstrations of quantum entanglement arising in a monitored Clifford circuit. It is worth recalling that recently [50] has reported an experimental demonstration of quantum error-correction properties (*i.e.* entanglement between the reference system R and the system) in a monitored Clifford circuit. Our main focus here is to directly verify quan-

tum entanglement in the system without using the reference system. We have also pointed out that a monitored circuit problem is fundamentally akin (or actually identical) to the Hayden-Preskill recovery problem by reversing the flow of time. The Hayden-Preskill recovery algorithm has been experimentally demonstrated, see [51, 52] for instance. We expect that similar experimental setups can be utilized to verify the entanglement structure in a monitored quantum circuit.

In this paper, we mainly focused on developing theoretical techniques to investigate the entanglement structure in monitored Clifford circuits without looking at specific models. The next step is to apply our framework to concrete models. A potentially interesting example is a random monitored Clifford circuit where both codeword and error vectors will have random entries which may give us some analytical control in computing coding properties. Also, we expect that our technique is useful in addressing the cases where the time evolution and measurements are translation symmetric in space and time. For such situations, polynomial representations of Pauli operators may be utilized [53, 54].

Another interesting future problem concerns the entanglement structure in generic monitored quantum circuits beyond Clifford dynamics. Naive applications of ideas from [17], or the Petz recovery map [15], would lead to a distillation algorithm which post-selects the measurement results to satisfy $m = \bar{m}$ (or in other words, $s = \bar{1}$). Unfortunately, the success probability will be rather small, and turning it into a deterministic algorithm will increase the circuit complexity by a huge factor. In this paper, for Clifford circuits, we have found that our entanglement distillation algorithm succeeds even without any feedback as long as $s = m \cdot \bar{m} \in \mathcal{E}$. This leaves a hope that the post-selection probability may not be pessimistically small for generic monitored circuits as well. Relatedly, we expect that modification of traversable wormhole protocols may provide efficient distillation methods [45–48].

It is interesting to note that insertion of boundaries (D -branes) in the AdS/BCFT correspondence has an effect similar to projecting a subsystem onto a random state [55, 56]. This suggests that insertion of boundaries may be interpreted as a projective measurement that realizes situations analogous to Eq. (138). It has been suggested that the effect of placing an end-of-the-world (EoW) brane on a two-sided AdS black hole is the same as projecting a quantum state to a particular pure quantum state [57]. It will be interesting to test this proposal further by using tensor network toy models [58, 59]. It is also useful to note that an effective action for entanglement entropy of monitored quantum circuits advocated in [22] (capillary-wave theory) contains a term which can be viewed as surface tension.

It is important to note that the volume-law entanglement exists because one records the measurement outcomes. If projective measurements were performed, but the measurement outcomes were forgotten, the total effect can be modelled as a dephasing channel. It will be interesting to consider the cases where measurement outcomes are partially forgotten. Our framework of mapping to a dual classical code may suggest a possibility that a little bit of forgetfulness can be tolerated when the encoding into codewords $\mathcal{C}(P_A)$ is robust.

As is evident from the construction of error vectors, the causal ordering of projective measurements P_1, \dots, P_r is crucial. Then, given a set of measured operators which are not necessarily sorted in a chronological order, it will be interesting to ask if the causal ordering (*i.e.* the arrow of time) can be inferred from the output wavefunction or not.

Acknowledgment

I thank Tim Hsieh and Zhi Li for useful discussions. Research at the Perimeter Institute is supported by the Government of Canada through Innovation, Science and Economic Development Canada and by the Province of Ontario through the Ministry of Economic Development, Job Creation and Trade.

A Measurement probability (Proof of lemma 1)

In this section, we prove lemma 1 by evaluating $\text{Prob}(m, \bar{m})$.

A.1 Measurement probability

Let us compute the probability of measuring m and \bar{m} . It is given graphically as follows:

$$\text{Prob}(m, \bar{m}) = \begin{array}{c} \begin{array}{cc} \Pi_1^\dagger(\bar{m}_1) & \Pi_1^T(\bar{m}_1) \\ \vdots & \vdots \\ \Pi_\tau^\dagger(\bar{m}_\tau) & \Pi_\tau^T(\bar{m}_\tau) \\ \vdots & \vdots \\ \Pi_1(m_1) & \Pi_1^*(m_1) \end{array} \\ \begin{array}{cc} A & B \\ B & A \end{array} \end{array} . \quad (163)$$

Here, in order to make the figure smaller, we moved some diagrams to the right hand side of the system. Specifically, we employed the following rule which applies to arbitrary operators:

$$\begin{array}{|c} \square \\ \hline \end{array} = \begin{array}{|c} \square^T \\ \hline \end{array} \quad (164)$$

where O^T represents a transpose of O .

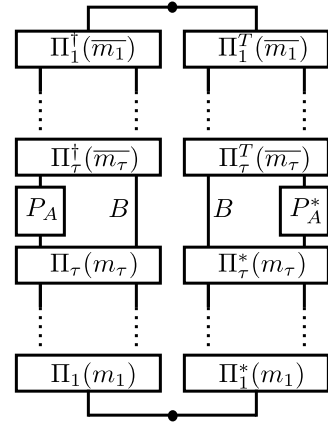
One can rewrite the above expression as follows:

$$\text{Prob}(m, \bar{m}) = \frac{1}{d_A^2} \sum_{P_A \in \text{Pauli}_A} \left\langle \Pi^\dagger(m) P_A^\dagger \Pi(\bar{m}) \Pi^\dagger(\bar{m}) P_A \Pi(m) \right\rangle \quad (165)$$

where we inserted the summation over Pauli operators on A , namely

$$\frac{1}{d_A} \sum_{P_A} P_A \otimes P_A^\dagger = \text{SWAP}_{A\bar{A}}. \quad (166)$$

Here it is convenient to introduce the following function:

$$\text{Prob}(m, \bar{m}; P_A) \equiv \left\langle \Pi^\dagger(m) P_A^\dagger \Pi(\bar{m}) \Pi^\dagger(\bar{m}) P_A \Pi(m) \right\rangle =$$


$$= \begin{array}{cc} \Pi_1^\dagger(\bar{m}_1) & \Pi_1^T(\bar{m}_1) \\ \vdots & \vdots \\ \Pi_\tau^\dagger(\bar{m}_\tau) & \Pi_\tau^T(\bar{m}_\tau) \\ P_A & B \\ \Pi_\tau(m_\tau) & \Pi_\tau^*(m_\tau) \\ \vdots & \vdots \\ \Pi_1(m_1) & \Pi_1^*(m_1) \end{array}. \quad (167)$$

Thus we arrived at the following lemma.

Lemma 7. *We have*

$$\text{Prob}(m, \bar{m}) = \frac{1}{d_A^2} \sum_{P_A \in \text{Pauli}_A} \text{Prob}(m, \bar{m}; P_A). \quad (168)$$

In other words, $\text{Prob}(m, \bar{m})$ is the average of $\text{Prob}(m, \bar{m}; P_A)$ taken over all the Pauli operators P_A on A .

The following lemma, concerning properties of $\text{Prob}(m, \bar{m}; P_A)$, will be useful.

Lemma 8. *We have*

$$\text{Prob}(m, \bar{m}; P_A) = \text{Prob}(m, \bar{m} \cdot \mathcal{C}(P_A); I_A). \quad (169)$$

The proof of lemma 8 is immediate from the following observation:

$$\Pi_j(m_j) P_A = P_A \Pi_j(m_j \cdot \mathcal{C}(P_A)_j) \quad (170)$$

since

$$P_j P_A = \mathcal{C}(P_A)_j P_A P_j \quad \mathcal{C}(P_A)_j = \pm 1. \quad (171)$$

Hence, we have

$$\begin{aligned} \text{Prob}(m, \bar{m}; P_A) &= \left\langle \Pi^\dagger(m) P_A^\dagger \Pi(\bar{m}) \Pi^\dagger(\bar{m}) P_A \Pi(m) \right\rangle \\ &= \left\langle \Pi^\dagger(m) \Pi(\bar{m} \cdot \mathcal{C}(P_A)) P_A^\dagger P_A \Pi^\dagger(\bar{m} \cdot \mathcal{C}(P_A)) \Pi(m) \right\rangle \\ &= \left\langle \Pi^\dagger(m) \Pi(\bar{m} \cdot \mathcal{C}(P_A)) \Pi^\dagger(\bar{m} \cdot \mathcal{C}(P_A)) \Pi(m) \right\rangle \\ &= \text{Prob}(m, \bar{m} \cdot \mathcal{C}(P_A); I_A). \end{aligned} \quad (172)$$

A.2 Summation of measurement probability

As we mentioned earlier, our primary focus will be on $s = m \cdot \bar{m}$. Hence it is convenient to define the summation of probabilities over m as follows:

$$\text{Sum}(s) \equiv \sum_m \text{Prob}(m, m \cdot s) \quad \text{Sum}(s; P_A) \equiv \sum_m \text{Prob}(m, m \cdot s; P_A). \quad (173)$$

We can verify

$$\text{Sum}(s) = \frac{1}{d_A^2} \sum_{P_A \in \text{Pauli}_A} \text{Sum}(s; P_A). \quad (174)$$

The central result of this section is the following lemma.

Lemma 9. *We have*

$$\begin{aligned} \text{Sum}(s; P_A) &\equiv \sum_m \text{Prob}(m, m \cdot s; P_A) = \frac{1}{d_{\mathcal{E}}} & s \in \mathcal{E}^{(P_A)} \\ &= 0 & s \notin \mathcal{E}^{(P_A)} \end{aligned} \quad (175)$$

where $d_{\mathcal{E}}$ is the number of elements in $\mathcal{E}^{(P_A)}$.

Due to lemma 8, it suffices to prove lemma 9 for $P_A = I_A$, namely

$$\text{Sum}(s; I_A) = \sum_m \text{Prob}(m, m \cdot s; I_A) = \frac{1}{d_{\mathcal{E}}} \quad s \in \mathcal{E}^{(I_A)}. \quad (176)$$

We will prove this statement in the next subsection.

With lemma 9 in hand, one can easily prove lemma 1. Namely, we have

$$\text{Sum}(s) = \frac{1}{d_A^2} \sum_{P_A \in \text{Pauli}_A} \text{Sum}(s; P_A). \quad (177)$$

Hence $\text{Sum}(s) = 0$ when $s \notin \mathcal{E}_{\text{total}}$. For $s \in \mathcal{E}_{\text{total}}$, $\text{Sum}(s)$ takes a uniform value. Hence we arrive at

$$\text{Sum}(s) = \frac{1}{d_{\mathcal{E}_{\text{total}}}} \quad s \in \mathcal{E}_{\text{total}}. \quad (178)$$

This completes the proof of lemma 1.

A.3 Proof of lemma 9

The proof of lemma 9 proceeds by induction, so it is convenient to denote the lemma with “ t -index”:

$$\text{Sum}^{(t)}(s^{(t)}; I_A) = \sum_{m^{(t)}} \text{Prob}^{(t)}(m^{(t)}, m^{(t)} \cdot s^{(t)}; I_A) = \frac{1}{d_{\mathcal{E}^{(t)}}} \quad s \in \mathcal{E}^{(t)} \quad (179)$$

for a monitored Clifford circuit with t measurements of P_1, \dots, P_t .

For $t = 1$, we have

$$\text{Prob}^{(1)}(m_1, \overline{m_1}; I_A) = \begin{array}{c} \begin{array}{cc} \Pi_1^\dagger(\overline{m_1}) & \Pi_1^T(\overline{m_1}) \\ \Pi_1(m_1) & \Pi_1^*(m_1) \end{array} \end{array} = \frac{1}{2} \delta_{m_1, \overline{m_1}} \quad (180)$$

and

$$\text{Sum}^{(1)}(s_1; I_A) = \sum_{m_1} \text{Prob}(m_1, \overline{m_1}; I_A) = \delta_{s_1, 1}. \quad (181)$$

The error vector set is given by $\mathcal{E}^{(1)} = \{(1)\}$ since $\mathcal{E}^{(1)}(P_1) = (1)$. So, the lemma holds for $t = 1$.

Next, let us assume that the lemma holds for $t = \tau - 1$ and show that the lemma holds also for $t = \tau$. We have

$$\text{Prob}^{(\tau)}(m^{(\tau)}, \overline{m}^{(\tau)}; I_A) = \begin{array}{c} \begin{array}{cc} \Pi_1^\dagger(\overline{m_1}) & \Pi_1^T(\overline{m_1}) \\ \vdots & \vdots \\ \Pi_\tau^\dagger(\overline{m_\tau}) & \Pi_\tau^T(\overline{m_\tau}) \\ \Pi_\tau(m_\tau) & \Pi_\tau^*(m_\tau) \\ \vdots & \vdots \\ \Pi_1(m_1) & \Pi_1^*(m_1) \end{array} \end{array} = \delta_{m_\tau, \overline{m_\tau}} \begin{array}{c} \begin{array}{cc} \Pi_1^\dagger(\overline{m_1}) & \Pi_1^T(\overline{m_1}) \\ \vdots & \vdots \\ \Pi_{\tau-1}^\dagger(\overline{m_{\tau-1}}) & \Pi_{\tau-1}^T(\overline{m_{\tau-1}}) \\ \Pi_\tau(m_\tau) & \Pi_\tau^*(m_\tau) \\ \Pi_{\tau-1}(m_{\tau-1}) & \Pi_{\tau-1}^*(m_{\tau-1}) \\ \vdots & \vdots \\ \Pi_1(m_1) & \Pi_1^*(m_1) \end{array} \end{array} \quad (182)$$

where $m^{(\tau)} = (m_1, \dots, m_\tau)$ and $\overline{m}^{(\tau)} = (\overline{m_1}, \dots, \overline{m_\tau})$. Here we used $\Pi_\tau^\dagger(\overline{m_\tau}) \Pi_\tau(m_\tau) = \delta_{m_\tau, \overline{m_\tau}} \Pi_\tau(m_\tau)$.

To compute $\text{Sum}^{(\tau)}(s^{(\tau)}; I_A)$, we set $\overline{m}^{(\tau)} = m^{(\tau)} \cdot s^{(\tau)}$ and sum over $m^{(\tau)}$. Summing over m_τ gives

$$\sum_{m_\tau} \text{Prob}^{(\tau)}(m^{(\tau)}, \overline{m}^{(\tau)}; I_A) = \delta_{s_\tau, 1} \sum_{m_\tau} \begin{array}{c} \begin{array}{cc} \Pi_1^\dagger(\overline{m_1}) & \Pi_1^T(\overline{m_1}) \\ \vdots & \vdots \\ \Pi_{\tau-1}^\dagger(\overline{m_{\tau-1}}) & \Pi_{\tau-1}^T(\overline{m_{\tau-1}}) \\ \Pi_\tau(m_\tau) & \Pi_\tau^*(m_\tau) \\ \Pi_{\tau-1}(m_{\tau-1}) & \Pi_{\tau-1}^*(m_{\tau-1}) \\ \vdots & \vdots \\ \Pi_1(m_1) & \Pi_1^*(m_1) \end{array} \end{array}. \quad (183)$$

Let us evaluate $\Pi_{\tau-1}^\dagger(\overline{m_{\tau-1}})\Pi_\tau(m_\tau)\Pi_{\tau-1}(m_{\tau-1})$. We have

$$\begin{aligned}\Pi_{\tau-1}^\dagger(\overline{m_{\tau-1}})\Pi_\tau(m_\tau)\Pi_{\tau-1}(m_{\tau-1}) &= \Pi_{\tau-1}^\dagger(\overline{m_{\tau-1}}) \left(\frac{I + m_\tau P_\tau}{2} \right) \Pi_{\tau-1}(m_{\tau-1}) \\ &= \frac{1}{2} \Pi_{\tau-1}^\dagger(\overline{m_{\tau-1}})\Pi_{\tau-1}(m_{\tau-1}) + \frac{m_1}{2} \Pi_{\tau-1}^\dagger(\overline{m_{\tau-1}})^\dagger P_\tau \Pi_{\tau-1}(m_{\tau-1}).\end{aligned}\quad (184)$$

Since $\Pi_{\tau-1}^\dagger(\overline{m_{\tau-1}})\Pi_\tau(m_\tau)\Pi_{\tau-1}(m_{\tau-1})$ appears twice in the expression of $\text{Prob}^{(\tau)}(m^{(\tau)}, \overline{m}^{(\tau)}; I_A)$, this decomposition generates four terms. Terms linear in m_τ will vanish when we take sum over m_τ . Hence we have

$$\begin{aligned}\sum_{m_\tau} \text{Prob}^{(\tau)}(m^{(\tau)}, \overline{m}^{(\tau)}; I_A) &= \frac{1}{2} \delta_{s_\tau, 1} \left(\begin{array}{c} \text{Diagram 1} + \text{Diagram 2} \end{array} \right) \\ &= \frac{1}{2} \delta_{s_\tau, 1} \left(\text{Prob}^{(\tau-1)}(m^{(\tau-1)}, \overline{m}^{(\tau-1)}; I_A) + \text{Prob}^{(\tau-1)}(m^{(\tau-1)}, \overline{m}^{(\tau-1)} \cdot \mathcal{E}(P_\tau)^{(\tau-1)}; I_A) \right).\end{aligned}\quad (185)$$

The diagrams are as follows:

Here we observed that the first diagram is identical to $\text{Prob}^{(\tau-1)}(m^{(\tau-1)}, \overline{m}^{(\tau-1)}; I_A)$ with $m^{(\tau-1)} = (m_1, \dots, m_{\tau-1})$ and $\overline{m}^{(\tau-1)} = (\overline{m_1}, \dots, \overline{m_{\tau-1}})$. As for the second diagram, commuting P_τ through and eliminating two P_τ 's change $\overline{m_j}$ as follows

$$\overline{m_j} \longrightarrow \overline{m_j} \cdot \mathcal{E}(P_\tau)_j \quad j = 1, \dots, \tau - 1. \quad (186)$$

So, the second diagram is identical to $\text{Prob}^{(\tau-1)}(m^{(\tau-1)}, \overline{m}^{(\tau-1)} \cdot \mathcal{E}(P_\tau)^{(\tau-1)}; I_A)$. Here we defined $\mathcal{E}(P_\tau)^{(\tau-1)}$ as a $\tau - 1$ -component vector:

$$\mathcal{E}(P_\tau)^{(\tau-1)} = (\mathcal{E}(P_\tau)_1, \dots, \mathcal{E}(P_\tau)_{\tau-1}) \quad (187)$$

by removing the τ -th component $\mathcal{E}(P_\tau)_\tau$.

By taking summation over $m_1, \dots, m_{\tau-1}$, we have

$$\text{Sum}^{(\tau)}(s^{(\tau)}; I_A) = \frac{1}{2} \delta_{s_\tau, 1} \left(\text{Sum}^{(\tau-1)}(s^{(\tau-1)}; I_A) + \text{Sum}^{(\tau-1)}(s^{(\tau-1)} \cdot \mathcal{E}(P_\tau)^{(\tau-1)}; I_A) \right). \quad (188)$$

By using the lemma for $t = \tau - 1$, we have

$$\text{Sum}^{(\tau-1)}(s^{(\tau-1)}; I_A) = \frac{1}{d_{\mathcal{E}^{(\tau-1)}}} \quad s^{(\tau-1)} \in \mathcal{E}^{(\tau-1)} \quad (189)$$

and

$$\text{Sum}^{(\tau-1)}(s^{(\tau-1)} \cdot \mathcal{E}(P_\tau)^{(\tau-1)}; I_A) = \frac{1}{d_{\mathcal{E}^{(\tau-1)}}} \quad s^{(\tau-1)} \cdot \mathcal{E}(P_\tau)^{(\tau-1)} \in \mathcal{E}^{(\tau-1)}. \quad (190)$$

The remaining task is to explicitly compute Eq. (188). It is convenient to consider two cases separately.

- If $\mathcal{E}(P_\tau)^{(\tau-1)} \in \mathcal{E}^{(\tau-1)}$, we have

$$d_{\mathcal{E}^{(\tau-1)}} = d_{\mathcal{E}^{(\tau)}} \quad (191)$$

and

$$\text{Sum}^{(\tau)}(s^{(\tau)}; I_A) = \delta_{s_\tau, 1} \text{Sum}^{(\tau-1)}(s^{(\tau-1)}; I_A) = \delta_{s_\tau, 1} \frac{1}{d_{\mathcal{E}^{(\tau-1)}}} = \delta_{s_\tau, 1} \frac{1}{d_{\mathcal{E}^{(\tau)}}} \quad s^{(\tau-1)} \in \mathcal{E}^{(\tau-1)}. \quad (192)$$

Note that $\text{Sum}^{(\tau)}(s^{(\tau)}; I_A)$ is nonzero only when $s_\tau = 1$, *i.e.*

$$s^{(\tau)} = (s_1, \dots, s_{\tau-1}, 1) \quad s^{(\tau-1)} \in \mathcal{E}^{(\tau-1)}. \quad (193)$$

This condition is equivalent to

$$s^{(\tau)} \in \mathcal{E}^{(\tau)} \quad (194)$$

since $\mathcal{E}(P_\tau)^{(\tau-1)} \in \mathcal{E}^{(\tau-1)}$. Hence, the lemma holds.

- If $\mathcal{E}(P_\tau)^{(\tau-1)} \notin \mathcal{E}^{(\tau-1)}$, we have

$$2d_{\mathcal{E}^{(\tau-1)}} = d_{\mathcal{E}^{(\tau)}} \quad (195)$$

and

$$\text{Sum}^{(\tau)}(s^{(\tau)}; I_A) = \frac{1}{2} \delta_{s_\tau, 1} \frac{1}{d_{\mathcal{E}^{(\tau-1)}}} = \delta_{s_\tau, 1} \frac{1}{d_{\mathcal{E}^{(\tau)}}} \quad s^{(\tau-1)} \in \mathcal{E}^{(\tau-1)} \quad \text{or} \quad s^{(\tau-1)} \in \mathcal{E}(P_\tau)^{(\tau-1)} \cdot \mathcal{E}^{(\tau-1)}. \quad (196)$$

The condition for nonzero $\text{Sum}^{(\tau)}(s^{(\tau)}; I_A)$ is equivalent to

$$s^\tau \in \mathcal{E}^{(\tau)}, \quad (197)$$

so, the lemma holds.

Hence, we have proved that the lemma holds for $t = \tau$ as well. This completes the proof of lemma 9 for arbitrary t by induction.

B Output of distillation algorithm (Proof of lemma 2)

In this section, we show that the aforementioned distillation algorithm outputs EPR pairs on $A\bar{A}$ when the classical error-correction condition is satisfied.

B.1 No feedback

We begin by discussing the cases where the measurement result satisfies $s = m \cdot \bar{m} \in \mathcal{E}^{(I_A)}$. For these cases, no feedback operation is needed. We explicitly find that the EPR fidelity is unity.

When the measurement outcome is m and \bar{m} , the EPR fidelity (an overlap with $|\text{EPR}\rangle_{A\bar{A}}$) is given by

$$F^{|\text{EPR}\rangle_{A\bar{A}}}(m, \bar{m}) = \frac{1}{d_A^2} \frac{\text{Prob}(m, \bar{m}; I_A)}{\text{Prob}(m, \bar{m})} \neq 0 \quad s \in \mathcal{E}^{(I_A)} \quad (198)$$

$$= 0 \quad s \notin \mathcal{E}^{(I_A)}$$

where the factor of $\text{Prob}(m, \bar{m})^{-1}$ comes from the normalization of the wavefunction. From lemma 9, we see that the fidelity is nonzero only when $s \in \mathcal{E}^{(I_A)}$. So, the cases with $s \notin \mathcal{E}^{(I_A)}$ will require some feedback operations.

The probability of measuring $s \in \mathcal{E}^{(I_A)}$ is given by

$$\sum_{s \in \mathcal{E}^{(I_A)}} \sum_m \text{Prob}(m, m \cdot s) = \sum_{s \in \mathcal{E}^{(I_A)}} \text{Sum}(s). \quad (199)$$

By post-selecting the measurement outcome to be $s \in \mathcal{E}^{(I_A)}$, the probability of having m, \bar{m} with $s \in \mathcal{E}^{(I_A)}$ is given by

$$\frac{\text{Prob}(m, \bar{m})}{\sum_{s \in \mathcal{E}^{(I_A)}} \text{Sum}(s)} \quad s \in \mathcal{E}^{(I_A)}. \quad (200)$$

The average fidelity is given by

$$\begin{aligned} \text{Fidelity} &= \sum_{s \in \mathcal{E}^{(I_A)}} \sum_m \frac{\text{Prob}(m, \bar{m})}{\sum_{s \in \mathcal{E}^{(I_A)}} \text{Sum}(s)} F^{|\text{EPR}\rangle_{A\bar{A}}}(m, \bar{m}) \\ &= \frac{1}{d_A^2} \frac{\sum_{s \in \mathcal{E}^{(I_A)}} \sum_m \text{Prob}(m, \bar{m}; I_A)}{\sum_{s \in \mathcal{E}^{(I_A)}} \text{Sum}(s)} \\ &= \frac{\sum_{s \in \mathcal{E}^{(I_A)}} \text{Sum}(s; I_A)}{\sum_{P_A \in \text{Pauli}_A} \sum_{s \in \mathcal{E}^{(I_A)}} \text{Sum}(s; P_A)} \\ &= 1 \end{aligned} \quad (201)$$

Here we used the error-correction condition. Namely, due to lemma 9, for $P_A \neq I_A$, we have

$$\text{Sum}(s; P_A) = 0 \quad s \in \mathcal{E}^{(I_A)}. \quad (202)$$

B.2 With feedback

Next, let us consider the cases where the measurement result satisfies $s = m \cdot \bar{m} \notin \mathcal{E}^{(I_A)}$. For these cases, we show that the output state, before applying the feedback, is given by the Choi-Jamiołkowski state $|P_A\rangle \equiv (P_A \otimes I_{\bar{A}})|\text{EPR}\rangle_{A\bar{A}}$. The fidelity for $|P_A\rangle$ is given by

$$F^{|P_A\rangle}(m, \bar{m}) = \frac{1}{d_A^2} \frac{\text{Prob}(m, \bar{m}; P_A)}{\text{Prob}(m, \bar{m})} \neq 0 \quad s \in \mathcal{E}^{(P_A)} \quad (203)$$

$$= 0 \quad s \notin \mathcal{E}^{(P_A)}.$$

By using lemma 8, we have

$$F^{|P_A\rangle}(m, \bar{m}) = \frac{1}{d_A^2} \frac{\text{Prob}(m, \bar{m} \cdot \mathcal{C}(P_A); I_A)}{\text{Prob}(m, \bar{m})}. \quad (204)$$

For $s \in \mathcal{E}^{(P_A)}$, we have

$$m \cdot \bar{m} \cdot \mathcal{C}(P_A) \in \mathcal{E}^{(I_A)}. \quad (205)$$

So, the calculation of Eq. (204) can be reduced to the case with $s \in \mathcal{E}^{(I_A)}$. Hence the average fidelity for $|P_A\rangle$ is unity. By applying the feedback Pauli operator P_A , we obtain $|I_A\rangle = |\text{EPR}\rangle$. Therefore, the aforementioned distillation algorithm outputs EPR pairs deterministically if the classical error-correction condition is satisfied.

B.3 Imperfect cases

We have shown that the distillation algorithm outputs EPR pairs deterministically when the classical error-correction condition is satisfied. Finally, we compute the output from the distillation algorithm when the condition is not satisfied.

Since the feedback operation effectively reduces the problem to the cases with $s \in \mathcal{E}^{(I_A)}$, it suffices to compute the output quantum state for $s \in \mathcal{E}^{(I_A)}$. We will explicitly decompose the output wavefunction by using the Choi-Jamiołkowski state of P_A . Namely, we will compute the overlap with $|P_A\rangle\langle Q_A|$ for $P_A, Q_A \in \text{Pauli}_A$. We have

$$F^{|P_A\rangle\langle Q_A|}(m, \bar{m}) = \frac{1}{\text{Prob}(m, \bar{m})} \frac{1}{d_A^2} \quad (206)$$

We begin with the cases with $P_A = Q_A$. We have

$$F^{|P_A\rangle\langle P_A|}(m, \bar{m}) = \frac{1}{d_A^2} \frac{\text{Prob}(m, \bar{m}; P_A)}{\text{Prob}(m, \bar{m})} \quad (s \in \mathcal{E}^{(I_A)}), \quad (207)$$

so the averaged fidelity is

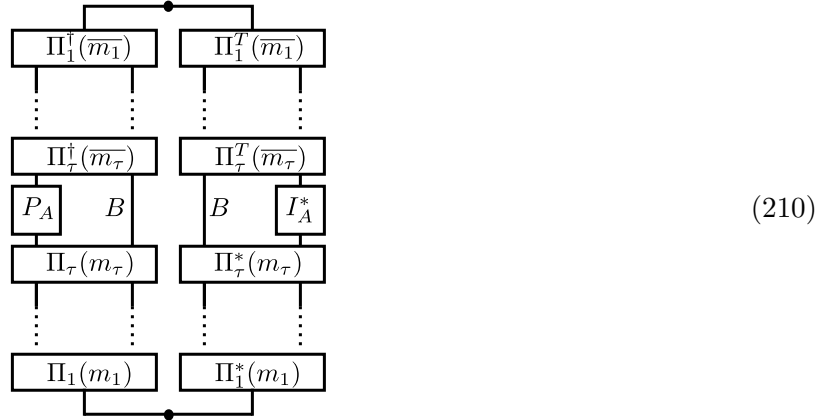
$$\text{Fidelity}^{|P_A\rangle\langle P_A|} = \frac{1}{d_A^2} \frac{\sum_{s \in \mathcal{E}^{(I_A)}} \text{Sum}(s; P_A)}{\sum_{s \in \mathcal{E}^{(I_A)}} \text{Sum}(s)} = \frac{\sum_{s \in \mathcal{E}^{(I_A)}} \text{Sum}(s; P_A)}{\sum_{P_A \in \text{Pauli}_A} \sum_{s \in \mathcal{E}^{(I_A)}} \text{Sum}(s; P_A)}. \quad (208)$$

Hence we have

$$\begin{aligned} \text{Fidelity}^{|P_A\rangle\langle P_A|} &= \frac{1}{N_{I_A}} & \mathcal{E}^{(P_A)} &= \mathcal{E}^{(I_A)} \\ &= 0 & \mathcal{E}^{(P_A)} &\neq \mathcal{E}^{(I_A)}. \end{aligned} \quad (209)$$

where N_{I_A} is the number of Pauli operators Q_A such that $\mathcal{E}^{(Q_A)} = \mathcal{E}^{(I_A)}$.

Next, we study the cases where $P_A \neq I_A$ and $Q_A = I_A$. The central object to study is the following diagram:



Recall that $\text{Tr}(P_A) = 0$ when $P_A \neq I$. Also recall that $\Pi_j(m_j)$ consists of an identity operator and a Pauli operator $m_j P_j$. So, in order to have a non-trivial contribution, some combinations of P_j 's in $\Pi(m), \Pi(\bar{m})$ need to generate P_A . In other words, there must exist a set of indices $\Lambda \in \{1, \dots, \tau\}$ such that

$$P_A \propto \prod_{j \in \Lambda} P_j \quad (211)$$

up to a $U(1)$ phase. In the above diagram, P_j appear four times. In order to generate a term proportional to P_A , P_j for $j \in \Lambda$ needs to be multiplied odd times because $P_j^2 = I$. Hence, possible coefficients of P_j are

$$m_j, \bar{m}_j, m_j^2 \bar{m}_j, m_j \bar{m}_j^2. \quad (212)$$

By fixing $s \in \mathcal{E}^{(I_A)}$, let us take summation over m . We see that terms with coefficients m_j and $m_j \bar{m}_j^2$

vanish. Also, since $\overline{m_j} = s_j \cdot m_j$, terms with coefficients $\overline{m_j}$ and $m_j^2 \overline{m_j}$ vanish. Hence we arrive at

$$\sum_{s \in \mathcal{E}^{(I_A)}} \sum_m \begin{array}{c} \begin{array}{|c|} \hline \Pi_1^I(\overline{m_1}) \\ \hline \vdots \\ \hline \Pi_{\tau-1}^I(\overline{m_{\tau-1}}) \\ \hline \Pi_{\tau-1}(\overline{m_{\tau-1}}) \\ \hline \vdots \\ \hline \Pi_1(m_1) \\ \hline \end{array} \quad \begin{array}{|c|} \hline \Pi_1^T(\overline{m_1}) \\ \hline \vdots \\ \hline \Pi_{\tau-1}^T(\overline{m_{\tau-1}}) \\ \hline \Pi_{\tau-1}^*(\overline{m_{\tau-1}}) \\ \hline \vdots \\ \hline \Pi_1^*(m_1) \\ \hline \end{array} \\ \hline \end{array} = 0 \quad (P_A \neq I_A). \quad (213)$$

So, there is no contribution to $|P_A\rangle\langle I_A|$ when $P_A \neq I_A$.

Finally, let us study the cases where $P_A \neq Q_A$. Since commuting Q_A through change \overline{m} to $\overline{m} \cdot \mathcal{C}(Q_A)$ and P_A to $P_A Q_A^\dagger$, the analysis from the previous paragraph (with $P_A \neq I_A$ and $Q_A = I_A$) can be applied. So, one can conclude that there is no contribution to $|P_A\rangle\langle Q_A|$ with $P_A \neq Q_A$. Hence, we arrive at

$$\rho_{A\overline{A}} = \frac{1}{N_{I_A}} \sum_{P_A: \mathcal{E}^{(P_A)} = \mathcal{E}^{(I_A)}} |P_A\rangle\langle P_A|. \quad (214)$$

This proves lemma 2.

C Conditional entropy (Proof of theorem 2)

In this section, we will compute the conditional entropy $S_{A|B} \equiv S_{AB} - S_B$.

The output of the monitored circuit is given by Eq. (12), which is reprinted below:

$$|\Psi(m)\rangle = \frac{1}{\sqrt{\text{Prob}(m)}} \begin{array}{c} \begin{array}{|c|} \hline A \\ \hline \end{array} \quad \begin{array}{|c|} \hline B \\ \hline \end{array} \quad \begin{array}{|c|} \hline R \\ \hline \end{array} \\ \hline \begin{array}{|c|} \hline \Pi_\tau(m_\tau) \\ \hline \vdots \\ \hline \Pi_2(m_2) \\ \hline \Pi_1(m_1) \\ \hline \end{array} \\ \hline \end{array} . \quad (215)$$

For an output of a Clifford circuit, it suffices to compute the Rényi-2 entropies. So, we have

$$2^{S_{A|B}(m)} = 2^{S_{AB}^{(2)}(m) - S_B^{(2)}(m)} = \frac{\text{Tr} [\rho_B(m)^2]}{\text{Tr} [\rho_{AB}(m)^2]}. \quad (216)$$

One can compute $\text{Tr} [\rho_B(m)^2]$ by looking at $\text{Prob}(m, m)$ (with $\overline{m} = m$). Namely we have the

following relation:

$$\text{Prob}(m, m) = \text{Tr} [\rho_B(m)^2] \text{Prob}(m)^2 \frac{d}{d_A}. \quad (217)$$

As for, $\text{Tr} [\rho_{AB}(m)^2]$, we have

$$\text{Prob}(m, m; I_A) = \text{Tr} [\rho_{AB}(m)^2] \text{Prob}(m)^2 d. \quad (218)$$

Hence, we have

$$2^{S_{A|B}(m)} = d_A \frac{\text{Prob}(m, m)}{\text{Prob}(m, m; I_A)}. \quad (219)$$

This equality holds as long as $\text{Prob}(m) \neq 0$.

We have obtained an expression of the conditional entropy $S_{A|B}(m)$ for each realization m . It turns out that $S_{A|B}(m)$ does not depend on m . This results from the following fact:

- Both $\text{Prob}(m, m; I_A)$ and $\text{Prob}(m, m)$ do not depend on m (as long as $\text{Prob}(m) \neq 0$).

This statement can be proven by using a certain property of Clifford circuits and stabilizer states. Here we sketch the proof idea. Recall that one can simulate the monitored Clifford circuit (consisting of Clifford gates with Pauli measurements) as a unitary Clifford circuit by adding ancilla qubits that record measurement results and entangling the circuit with ancilla qubits by Control-Not gates (which are Clifford operators). For instance, the output from the monitored circuit with ancilla qubits can be written as

$$\sum_m \sqrt{\text{Prob}(m)} |\Psi(m)\rangle \otimes |m\rangle \quad (220)$$

where $|m\rangle = |m_1, \dots, m_\tau\rangle$ is defined on τ ancilla qubits. Note that the above quantum state is a stabilizer state, so its spectrum of reduced density matrices in subsystems must be flat (which can be proven in a standard manner, see [60] for instance). Looking at the reduced density matrix on the ancilla Hilbert space, its coefficient for $|m\rangle\langle m|$ corresponds to $\text{Prob}(m)$ which must be uniform as long as $\text{Prob}(m) \neq 0$:

$$\text{Prob}(m) = \text{const} \quad \text{if} \quad \text{Prob}(m) \neq 0. \quad (221)$$

Similarly, one can construct stabilizer states whose reduced density matrices encode $\text{Prob}(m, m; I_A)$ and $\text{Prob}(m, m)$ as coefficients. Then we can prove that $\text{Prob}(m, m; I_A)$ and $\text{Prob}(m, m)$ are uniform and do not depend on m .

By using this property of Clifford quantum circuits, we arrive at

$$\begin{aligned} 2^{S_{A|B}(m)} &= d_A \frac{\text{Sum}(s=1)}{\text{Sum}(s=1; I_A)} \\ &= \frac{1}{d_A} \frac{\sum_{P_A \in \text{Pauli}_A} \text{Sum}(s=1; P_A)}{\text{Sum}(s=1; I_A)} \\ &= \frac{N_{I_A}}{d_A}. \end{aligned} \quad (222)$$

This completes the proof of theorem 2).

D Logical operators (Proof of lemma 4)

In this section, we will prove

$$\mathcal{C}(P) \in \mathcal{E}^{(I)} \Leftrightarrow P \in \mathcal{L}. \quad (223)$$

The proof proceeds by induction. It is immediate to show that Eq. (223) holds for $\tau = 1$ as $\text{Logic}^{(1)}$ is defined as the commutant of P_1 . Here we assume that Eq. (223) holds for $\tau - 1$ and prove it for τ .

Proof of \Leftarrow : Let us assume $P \in \text{Logic}^{(\tau)}$ and prove $\mathcal{C}(P) \in \mathcal{E}^{(I)}$. It is useful to recall that if $P \in \text{Logic}^{(\tau)}$, then $[P, P_\tau] = 0$ since $P_\tau \in \text{Stab}^{(\tau)}$.

- Case 1: $P \in \text{Logic}^{(\tau-1)}$.

In this case, we have $[P, P_\tau] = [P, P_{\tau-1}] = 0$, so $\mathcal{C}(P)$'s entries for the τ -th and $\tau-1$ -th components are trivial. By using Eq. (223) for $\tau-1$, we see that there exists a set of indices $\Lambda \subseteq \{1, \dots, \tau-1\}$ such that

$$\mathcal{C}(P) = \prod_{j \in \Lambda} \mathcal{E}(P_j) \in \mathcal{E}^{(I)}. \quad (224)$$

- Case 2: $P \notin \text{Logic}^{(\tau-1)}$.

In this case, with some work, one can prove $PP_\tau \in \text{Logic}^{(\tau-1)}$ ¹⁸.

Since $PP_\tau \in \text{Logic}^{(\tau)}$, one can apply the argument from Case 1 to PP_τ . This shows

$$\mathcal{C}(PP_\tau) \in \mathcal{E}^{(I)}. \quad (225)$$

Since $\mathcal{C}(P_\tau) \in \mathcal{E}^{(I)}$, we have $\mathcal{C}(P) \in \mathcal{E}^{(I)}$.

Proof of \Rightarrow : Let us assume $\mathcal{C}(P) \in \mathcal{E}^{(I)}$ and prove $P \in \text{Logic}^{(\tau)}$. From this assumption, there exists a set of indices $\Lambda \in \{1, \dots, \tau\}$ such that

$$\mathcal{C}(P) = \prod_{j \in \Lambda} \mathcal{E}(P_j). \quad (226)$$

- Case 1: $\tau \notin \Lambda$.

¹⁸Recall that $P \in \text{Logic}^{(\tau)}$ implies that P commutes with all the elements in $\text{Stab}^{(\tau)}$ since $\text{Logic}^{(\tau)}$ is the commutant of $\text{Stab}^{(\tau)}$. But $P \notin \text{Logic}^{(\tau-1)}$ implies that P does not commute with some elements in $\text{Stab}^{(\tau-1)}$. Here we can write independent stabilizer generators as $\text{Stab}^{(\tau-1)} = \langle S_1, S_2, \dots \rangle$ such that $[P, S_1] \neq 0$ and $[P, S_j] = 0$ for $j \geq 2$.

Now, we prove $[P_\tau, S_1] \neq 0$ and $[P_\tau, S_j] = 0$ for $j \geq 2$. Let us begin with $[P_\tau, S_1] \neq 0$. Suppose $[P_\tau, S_1] = 0$. Then, from the recursive construction of $\text{Stab}^{(\tau)}$, we see that $S_1 \in \text{Stab}^{(\tau)}$. This contradicts with the fact that $[P, S_1] \neq 0$, but $[P, \text{Stab}^{(\tau)}] = 0$. So, we have $[P_\tau, S_1] \neq 0$.

As for $[P_\tau, S_j] = 0$ for $j \geq 2$, let us focus on $j = 2$. Suppose $[P_\tau, S_2] \neq 0$. Then we have $[P_\tau, S_1 S_2] = 0$ which implies $S_1 S_2 \in \text{Stab}^{(\tau)}$. But this contradicts with the fact that $[P, S_1] \neq 0$ and $[P, S_2] = 0$, but P commutes with all the elements in $\text{Stab}^{(\tau)}$. So we have $[P_\tau, S_j] = 0$ for $j \geq 2$.

From these arguments, one can show that $PP_\tau \in \text{Logic}^{(\tau-1)}$.

In this case, by using Eq. (223) for $\tau - 1$, we see that $P \in \text{Logic}^{(\tau-1)}$. Eq. (226) implies that the τ -th component of $\mathcal{C}(P)$ is trivial, and hence $[P, P_\tau] = 0$. This implies

$$P \in \text{Logic}^{(\tau)}. \quad (227)$$

- Case 2: $\tau \in \Lambda$.

In this case, we observe

$$\mathcal{C}(PP_\tau) = \prod_{j \in \Lambda/\tau} \mathcal{E}(P_j). \quad (228)$$

where Λ/τ means that τ is removed from Λ . Then, one can apply the argument from Case 1 to PP_τ . This completes the proof.

E More on coding properties

In this appendix, we present additional results on the coding properties of a monitored Clifford circuit as well as proofs of some technical results.

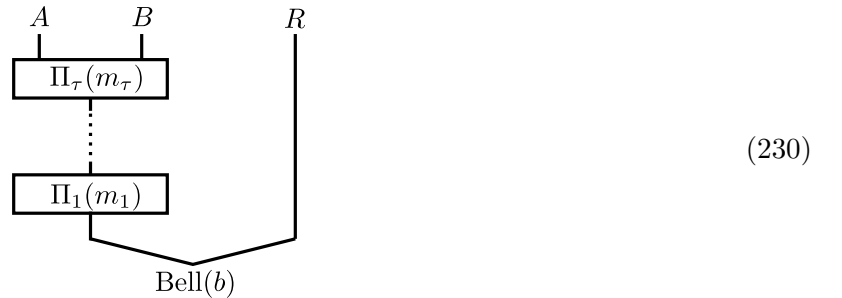
E.1 Extended codewords

In this subsection, we will present an alternative derivation of the entanglement structure by treating the reference system R as a part of the system.

Instead of treating AB as a system, we think of ABR as the whole system. Specifically, imagine that there were initially $2n$ qubits in maximally mixed states and we perform Bell measurements in the following $2n$ Bell operators:

$$X_j^{AB} \otimes X_j^R \quad Z_j^{AB} \otimes Z_j^R \quad j = 1, \dots, n. \quad (229)$$

This will create a maximally entangled state on ABR . We then proceed to perform projective measurements $\Pi(m)$ on A . In this interpretation, the reference R becomes a part of the system and we have a $2n$ -qubit monitored quantum circuit where original P_j measurements, as well as Bell measurements, are performed:



where $\text{Bell}(b)$ represent Bell measurements with outcomes b . Starting from EPR pairs between AB and R is equivalent to postselecting the measurement outcomes to satisfy $b = (1, \dots, 1)$.

In total, $\tau + 2n$ measurements are performed. Here it is convenient to define extended codeword and error vectors which include Bell measurements. Namely, we introduce an extended measurement vector

$$m_{\text{ext}} \equiv (m, b) \quad (231)$$

which has $\tau + 2n$ components. We can also define extended codeword and error vectors by $\mathcal{C}_{\text{ext}}(P_A)$ and $\mathcal{E}_{\text{ext}}(P_j)$ that account for commutation relations with respect to $2n$ Bell measurement operators as well as the original projective measurements of P_j . Extended error sets are denoted by $\mathcal{E}_{\text{ext}}^{(P_A)}$ with the error set $\mathcal{E}_{\text{ext}} = \mathcal{E}_{\text{ext}}^{(I_A)}$.

One can compute entanglement entropies of subsystems in terms of these extended vectors. By choosing Pauli operators on A , B and AB as initial information of the extended classical error-correcting code, we obtain the following three relations:

$$\begin{aligned} S_{A|BR} &= -S_A = \log N_{I_{A\text{ext}}} - n_A & N_{I_{A\text{ext}}} &: \text{number of } P_A \text{ s.t. } \mathcal{C}_{\text{ext}}(P_A) \in \mathcal{E}_{\text{ext}}. \\ S_{B|AR} &= -S_B = \log N_{I_{B\text{ext}}} - n_B & N_{I_{B\text{ext}}} &: \text{number of } P_B \text{ s.t. } \mathcal{C}_{\text{ext}}(P_B) \in \mathcal{E}_{\text{ext}}. \\ S_{AB|R} &= -S_R = \log N_{I_{\text{ext}}} - n & N_{I_{\text{ext}}} &: \text{number of } P \text{ s.t. } \mathcal{C}_{\text{ext}}(P) \in \mathcal{E}_{\text{ext}}. \end{aligned} \quad (232)$$

It will be convenient to define the following three sets of Pauli operators:

$$\begin{aligned} \mathcal{S} &\equiv \{P \in \text{Pauli} : \mathcal{C}(P) \in \mathcal{E}\} \\ \mathcal{S}_A &\equiv \{P_A \in \text{Pauli}_A : \mathcal{C}(P_A) \in \mathcal{E}\}. \\ \mathcal{S}_B &\equiv \{P_B \in \text{Pauli}_B : \mathcal{C}(P_B) \in \mathcal{E}\} \end{aligned} \quad (233)$$

Expert readers will recognize that Eq. (232) is identical to the well-known formula for the entanglement entropy for a stabilizer state [60]:

$$S_R = n_R - \log |\mathcal{S}_R| \quad (234)$$

where R is an arbitrary subsystem and \mathcal{S}_R is the restriction of the stabilizer group \mathcal{S} onto R . Later, we will indeed show that these Pauli operators in \mathcal{S} serve as stabilizer generators when the monitored Clifford circuit is viewed as a quantum error-correcting code. Using these relations, we obtain

$$\begin{aligned} I_{(A,B)} &= \log \frac{N_{I_{\text{ext}}}}{N_{I_{A\text{ext}}} N_{I_{B\text{ext}}}} \\ S_{AB|R} &= \log_2 N_{I_{\text{ext}}} - n. \end{aligned} \quad (235)$$

E.2 Stabilizer operator from extended code

The following lemma can be proven in a way similar to lemma 4.

Lemma 10. *Null operators in the extended code are stabilizer operators. Namely we have*

$$\mathcal{C}_{\text{ext}}(P) \in \mathcal{E}_{\text{ext}} \quad \text{iff} \quad P \in \mathcal{S}. \quad (236)$$

We will skip the proof. Our findings so far are summarized in Fig. 6.

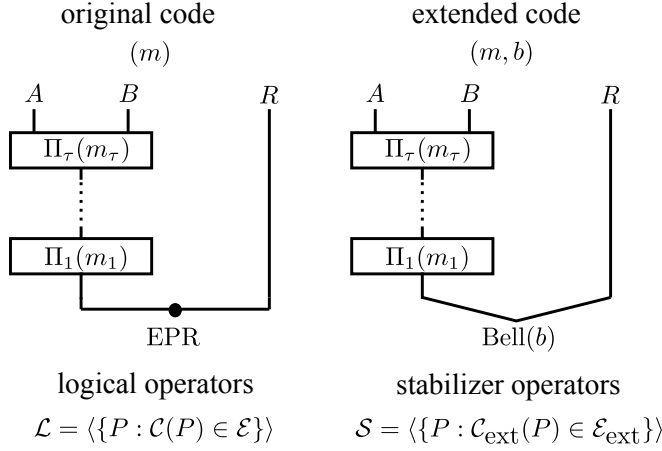


Figure 6: The original dual code and the extended dual code. The extended dual code is constructed by viewing ABR , including the reference R , as a whole system. Null vectors in two codes become logical operators and stabilizer operators.

E.3 Cleaning lemma for monitored circuit

We presented two different derivations of entanglement entropies by using the original and extended codewords respectively. This suggests that the numbers of Pauli operators in the logical operator groups (N_I, N_{I_A}, N_{I_B}) and those in the stabilizer group $(N_{I_{\text{ext}}}, N_{I_{A_{\text{ext}}}}, N_{I_{B_{\text{ext}}}})$ can be related. Here we find the following three independent constraints:

$$\log N_I + \log N_{I_A} + \log N_{I_B} = \log N_{I_{\text{ext}}} + \log N_{I_{A_{\text{ext}}}} + \log N_{I_{B_{\text{ext}}}} \quad (237)$$

$$\log N_{I_A} = 2n_A - \log N_{I_{\text{ext}}} + \log N_{I_{B_{\text{ext}}}} \quad (238)$$

$$\log N_{I_B} = 2n_B - \log N_{I_{\text{ext}}} + \log N_{I_{A_{\text{ext}}}}. \quad (239)$$

Below, we present coding theoretic interpretations of these equations.

Let us begin with Eq. (237). Recall that $\log N_{I_{\text{ext}}}$ is the number of independent stabilizer generators in \mathcal{S} . Also observe that $\log N_I$ is the number of independent stabilizer generators as well as independent logical operators. So, we have

$$g \equiv \log N_I - \log N_{I_{\text{ext}}} = \text{number of independent logical operators.} \quad (240)$$

Similarly, we find

$$\begin{aligned} g_A &\equiv \log N_{I_A} - \log N_{I_{A_{\text{ext}}}} = \text{number of independent logical operators supported on } A \\ g_B &\equiv \log N_{I_B} - \log N_{I_{B_{\text{ext}}}} = \text{number of independent logical operators supported on } B. \end{aligned} \quad (241)$$

With these interpretations, Eq. (237) can be rewritten as

$$g_A + g_B = g. \quad (242)$$

Noting that $g = 2k$ where k is the number of logical qubits, this equation is identical to the cleaning lemma from [34].

Next, we look at Eq. (238). Let us compute N_{I_A} (the number of elements in \mathcal{L}_A) explicitly. Recall

that logical operators on A commute with all the stabilizer generators. Since they are supported exclusively on A , it suffices to look at independent stabilizer generators which have supports on A . In total, there are $\log N_{I_{\text{ext}}} - \log N_{I_{B_{\text{ext}}}}$ independent stabilizer generators with non-trivial supports on A . Recalling that there are $2n_A$ independent Pauli operators on A , we find

$$\log N_{I_A} = 2n_A - (\log N_{I_{\text{ext}}} - \log N_{I_{B_{\text{ext}}}}) \quad (243)$$

which is identical to Eq. (238). Hence, Eq. (238) can be interpreted as a formula to compute the number of logical operators supported on A . Eq. (239) has a similar interpretation for logical operators on B .

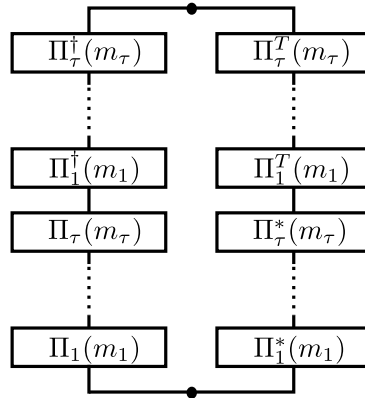
Another interesting relation, which can be derived from the aforementioned three relations, is

$$\log N_I + \log N_{I_{\text{ext}}} = 2n. \quad (244)$$

This follows from the fact that the logical operator group \mathcal{L} is the commutant of \mathcal{S} (and vice versa).

E.4 Measurement probability (Proof of lemma 5)

In the system-reference entanglement distillation algorithm, the probability of measuring m and \bar{m} is given by



$$\quad (245)$$

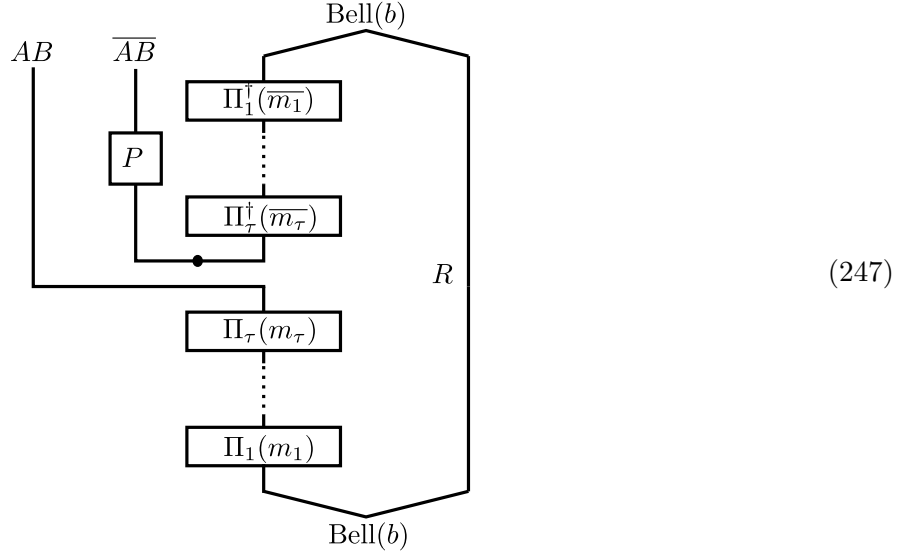
Observe that this quantity is identical to $\text{Prob}(m, \bar{m}; I_A)$ in Eq. (167) with P_τ, \dots, P_1 arranged in the reverse chronological order. Then, from lemma 9, we can show that one may measure $s = m \cdot \bar{m}$ if and only if

$$s \in \mathcal{E}_{\text{rev}}. \quad (246)$$

This proves lemma 5.

E.5 Entanglement distillation from reference (Proof of lemma 6)

By treating the reference R as a part of the system, one can utilize the algorithm from section 4 to distill entanglement between AB and R . The whole procedure is graphically summarized as follows:



where $\text{Bell}^\dagger(\bar{b})$ represent the reverse Bell measurements with outcomes \bar{b} . Note that we can set $b = (1, \dots, 1)$ by preparing EPR pairs on ABR at the beginning, instead of performing Bell measurements.

The distillation algorithm proceeds by finding an appropriate feedback Pauli operator. Let us introduce the following extended vectors:

$$\bar{m}_{\text{ext}} \equiv (\bar{m}, \bar{b}) \quad s_{\text{ext}} \equiv (s, b \cdot \bar{b}). \quad (248)$$

Then, after performing the aforementioned protocol, we compute s_{ext} and solve for P satisfying

$$s_{\text{ext}} \in \mathcal{E}_{\text{ext}}^{(P)}. \quad (249)$$

By using lemma 2, we notice that the output of the distillation algorithm, averaged over the measurement outcomes, is given by

$$\mathbb{E}(\sigma_{AB\bar{A}\bar{B}}) = \frac{1}{N_{I_{\text{ext}}}} \sum_{P \in \mathcal{S}} |P\rangle\langle P| \quad (250)$$

where $N_{I_{\text{ext}}}$ is the number of Pauli operators which satisfy $\mathcal{C}_{\text{ext}}(P) \in \mathcal{E}_{\text{ext}}$ (*i.e.* the number of elements in \mathcal{S}). From this expression, one may see that \mathcal{S} indeed plays the role of the stabilizer group.

Finally, let us prove lemma 6. Recall that the feedback operator in the aforementioned distillation algorithm reduces the system to the situations with $m = \bar{m}$ and $b = \bar{b}$. Also observe that this entanglement distillation in Eq. (247) is identical to the one from the main part of the paper in Eq. (117) when $b = \bar{b}$. Hence, it suffices to prove that the feedback operation for the algorithm in Eq. (117) reduces the system to the situations with $m = \bar{m}$.

This can be proven from the following observation:

$$P_j \Pi(m) = P_j \frac{I + m_\tau P_\tau}{2} \dots \frac{I + m_j P_j}{2} \dots \frac{I + m_1 P_1}{2} = m_j \Pi(m \cdot \mathcal{E}_{\text{rev}}(P_j)). \quad (251)$$

So, we have

$$P_\Lambda \Pi(m) \propto \Pi(m \cdot \mathcal{E}_{\text{rev}}(P_\Lambda)). \quad (252)$$

Hence, applying P_Λ reduces the system to the situation with $m = \bar{m}$. Thus, the output of the distillation algorithm from section 7 outputs the quantum state in Eq. (250). This proves lemma 6.

References

- [1] Y. Li, X. Chen, and M. P. A. Fisher, “Quantum zeno effect and the many-body entanglement transition,” *Phys. Rev. B* **98** (2018) 205136.
- [2] B. Skinner, J. Ruhman, and A. Nahum, “Measurement-induced phase transitions in the dynamics of entanglement,” *Phys. Rev. X* **9** (2019) 031009.
- [3] M. Ippoliti, M. J. Gullans, S. Gopalakrishnan, D. A. Huse, and V. Khemani, “Entanglement phase transitions in measurement-only dynamics,” *Phys. Rev. X* **11** (2021) 011030.
- [4] C.-M. Jian, Y.-Z. You, R. Vasseur, and A. W. W. Ludwig, “Measurement-induced criticality in random quantum circuits,” *Phys. Rev. B* **101** (2020) 104302.
- [5] A. Lavasani, Y. Alavirad, and M. Barkeshli, “Measurement-induced topological entanglement transitions in symmetric random quantum circuits,” *Nature Physics* **17** (2021) 342.
- [6] A. Zabalo, M. J. Gullans, J. H. Wilson, S. Gopalakrishnan, D. A. Huse, and J. H. Pixley, “Critical properties of the measurement-induced transition in random quantum circuits,” *Phys. Rev. B* **101** (2020) 060301–.
- [7] M. Szyniszewski, A. Romito, and H. Schomerus, “Entanglement transition from variable-strength weak measurements,” *Phys. Rev. B* **100** (2019) 064204.
- [8] S. Sang and T. H. Hsieh, “Measurement-protected quantum phases,” *Phys. Rev. Res.* **3** (2021) 023200.
- [9] Y. Li, X. Chen, A. W. W. Ludwig, and M. P. A. Fisher, “Conformal invariance and quantum non-locality in hybrid quantum circuits,” [arXiv:2003.12721](https://arxiv.org/abs/2003.12721).
- [10] A. Nahum, S. Roy, B. Skinner, and J. Ruhman, “Measurement and entanglement phase transitions in all-to-all quantum circuits, on quantum trees, and in landau-ginsburg theory,” *PRX Quantum* **2** (2021) 010352.
- [11] S. Vijay, “Measurement-driven phase transition within a volume-law entangled phase,” [arXiv:2005.03052](https://arxiv.org/abs/2005.03052).

- [12] L. Zhang, J. A. Reyes, S. Kourtis, C. Chamon, E. R. Mucciolo, and A. E. Ruckenstein, “Nonuniversal entanglement level statistics in projection-driven quantum circuits,” *Phys. Rev. B* **101** (2020) 235104.
- [13] Q. Tang and W. Zhu, “Measurement-induced phase transition: A case study in the nonintegrable model by density-matrix renormalization group calculations,” *Phys. Rev. Res.* **2** (2020) 013022.
- [14] Y. Bao, S. Choi, and E. Altman, “Theory of the phase transition in random unitary circuits with measurements,” *Phys. Rev. B* **101** (2020) 104301.
- [15] M. Ohya and D. Petz, *Quantum Entropy and Its Use*. Springer-Verlag, Berlin, 1993.
- [16] B. Yoshida. In preparation.
- [17] B. Yoshida and A. Kitaev, “Efficient decoding for the hayden-preskill protocol,” [arXiv:1710.03363](#).
- [18] S. Choi, Y. Bao, X.-L. Qi, and E. Altman, “Quantum error correction in scrambling dynamics and measurement-induced phase transition,” *Phys. Rev. Lett.* **125** (2020) 030505.
- [19] M. J. Gullans and D. A. Huse, “Dynamical purification phase transition induced by quantum measurements,” *Phys. Rev. X* **10** (2020) 041020.
- [20] M. J. Gullans and D. A. Huse, “Scalable probes of measurement-induced criticality,” *Phys. Rev. Lett.* **125** (2020) 070606.
- [21] R. Fan, S. Vijay, A. Vishwanath, and Y.-Z. You, “Self-organized error correction in random unitary circuits with measurement,” *Phys. Rev. B* **103** (2021) 174309.
- [22] Y. Li and M. P. A. Fisher, “Statistical mechanics of quantum error correcting codes,” *Phys. Rev. B* **103** (2021) 104306.
- [23] L. Fidkowski, J. Haah, and M. B. Hastings, “How dynamical quantum memories forget,” *Quantum* **5** (2021) 382.
- [24] M. Ippoliti and V. Khemani, “Postselection-free entanglement dynamics via spacetime duality,” *Phys. Rev. Lett.* **126** (2021) 060501.
- [25] B. Yoshida, “Decoding algorithms for clifford hayden-preskill problem,” [arXiv:2106.15628](#).
- [26] B. Yoshida, “Observer-dependent black hole interior from operator collision,” *Phys. Rev. D* **103** (2021) 046004.
- [27] Y. Sekino and L. Susskind, “Fast scramblers,” *JHEP* **10** (2008) 065.
- [28] P. W. Shor, “Scrambling time and causal structure of the photon sphere of a schwarzschild black hole,” [arXiv:1807.04363](#).
- [29] P. Hosur, X.-L. Qi, D. A. Roberts, and B. Yoshida, “Chaos in quantum channels,” *JHEP* **02** (2016) 004.
- [30] A. Kitaev. Unpublished.

- [31] D. A. Roberts, D. Stanford, and L. Susskind, “Localized shocks,” *JHEP* **3** (2015) 51.
- [32] B. Yoshida, “Soft mode and interior operator in the hayden-preskill thought experiment,” *Phys. Rev. D* **100** (2019) 086001.
- [33] S. Bravyi and B. Terhal, “A no-go theorem for a two-dimensional self-correcting quantum memory based on stabilizer codes,” *New. J. Phys.* **11** (2009) 043029.
- [34] B. Yoshida and I. L. Chuang, “Framework for classifying logical operators in stabilizer codes,” *Phys. Rev. A* **81** (2010) 052302.
- [35] P. Hayden, M. Horodecki, A. Winter, and J. Yard, “A decoupling approach to the quantum capacity,” *Open Syst. Inf. Dyn.* **15** (2008) 7.
- [36] B. Yoshida and N. Y. Yao, “Disentangling scrambling and decoherence via quantum teleportation,” *Phys. Rev. X* **9** (2019) 011006.
- [37] B. Schumacher and M. D. Westmoreland, “Approximate quantum error correction,” *Quantum Inf. Process.* **1** (2002) 5.
- [38] Y. Li, S. Vijay, and M. P. A. Fisher, “Entanglement domain walls in monitored quantum circuits and the directed polymer in a random environment,” [arXiv:2105.13352](#).
- [39] B. Yoshida, “Remarks on black hole complexity puzzle,” *JHEP* **10** (2020) 103.
- [40] Y. Li, X. Chen, and M. P. A. Fisher, “Measurement-driven entanglement transition in hybrid quantum circuits,” *Phys. Rev. B* **100** (2019) 134306.
- [41] P. Hayden and J. Preskill, “Black holes as mirrors: quantum information in random subsystems,” *JHEP* **09** (2007) 120.
- [42] D. A. Roberts and B. Yoshida, “Chaos and complexity by design,” *JHEP* **4** (2017) 121.
- [43] P. Gao, D. L. Jafferis, and A. C. Wall, “Traversable wormholes via a double trace deformation,” *JHEP* **12** (2017) 151.
- [44] J. Maldacena, D. Stanford, and Z. Yang, “Diving into traversable wormholes,” *Fortsch. Phys.* **65** (2017) 1700034.
- [45] A. R. Brown, H. Gharibyan, S. Leichenauer, H. W. Lin, S. Nezami, G. Salton, L. Susskind, B. Swingle, and M. Walter, “Quantum gravity in the lab: Teleportation by size and traversable wormholes,” [arXiv:1911.06314](#).
- [46] S. Nezami, H. W. Lin, A. R. Brown, H. Gharibyan, S. Leichenauer, G. Salton, L. Susskind, B. Swingle, and M. Walter, “Quantum gravity in the lab: Teleportation by size and traversable wormholes, part ii,” [arXiv:2102.01064](#).
- [47] P. Gao and D. L. Jafferis, “A traversable wormhole teleportation protocol in the syk model,” [arXiv:1911.07416](#).

- [48] T. Schuster, B. Kobrin, P. Gao, I. Cong, E. T. Khabiboulline, N. M. Linke, M. D. Lukin, C. Monroe, B. Yoshida, and N. Y. Yao, “Many-body quantum teleportation via operator spreading in the traversable wormhole protocol,” [arXiv:2102.00010](#).
- [49] B. Yoshida, “Firewalls vs. scrambling,” *JHEP* **10** (2019) 132.
- [50] C. Noel, P. Niroula, D. Zhu, A. Risinger, L. Egan, D. Biswas, M. Cetina, A. V. Gorshkov, M. J. Gullans, D. A. Huse, and C. Monroe, “Observation of measurement-induced quantum phases in a trapped-ion quantum computer,” [arXiv:2106.05881](#).
- [51] K. A. Landsman, C. Figgatt, T. Schuster, N. M. Linke, B. Yoshida, N. Y. Yao, and C. Monroe, “Verified quantum information scrambling,” *Nature* **567** (2019) 61.
- [52] M. S. Blok, V. V. Ramasesh, T. Schuster, K. O’Brien, J. M. Kreikebaum, D. Dahlen, A. Morvan, B. Yoshida, N. Y. Yao, and I. Siddiqi, “Quantum information scrambling on a superconducting qutrit processor,” *Phys. Rev. X* **11** (2021) 021010.
- [53] J. Haah, “Commuting pauli hamiltonians as maps between free modules,” *Comm. Math. Phys.* **324** (2013) 351.
- [54] B. Yoshida, “Exotic topological order in fractal spin liquids,” *Phys. Rev. B* **88** (2013) 125122.
- [55] T. Takayanagi, “Holographic dual of a boundary conformal field theory,” *Phys. Rev. Lett.* **107** (2011) 101602.
- [56] M. Fujita, T. Takayanagi, and E. Tonni, “Aspects of ads/bcft,” *JHEP* **11** (2011) 43.
- [57] A. Almheiri, “Holographic quantum error correction and the projected black hole interior,” [arXiv:1810.02055](#).
- [58] F. Pastawski, B. Yoshida, D. Harlow, and J. Preskill, “Holographic quantum error-correcting codes: toy models for the bulk/boundary correspondence,” *JHEP* **06** (2015) 149.
- [59] P. Hayden, S. Nezami, X.-L. Qi, N. Thomas, M. Walter, and Z. Yang, “Holographic duality from random tensor networks,” *JHEP* **11** (2016) 9.
- [60] D. Fattal, T. S. Cubitt, Y. Yamamoto, S. Bravyi, and I. L. Chuang, “Entanglement in the stabilizer formalism,” [quant-ph/0406168](#).